Supporting Information

Highly fluorescent covalent organic framework as hydrogen chloride sensor: Roles of Schiff base bonding and π-stacking

Ahmed F. M. EL-Mahdy,[a,*] Ming-Yi Lai,[a] and Shiao-Wei Kuo[a,b,*]

[a]Department of Materials and Optoelectronic Science, Center of Crystal Research, National Sun Yat-Sen University, Kaohsiung, 80424, Taiwan

[b]Department of Medicinal and Applied Chemistry, Kaohsiung Medical University, Kaohsiung, 807, Taiwan

*To whom correspondence should be addressed

E-mail: ahmed1932005@gmail.com and kuosw@faculty.nsysu.edu.tw

TEL./FAX: 886-7-5254099

S1. Materials

Chemicals and solvents were obtained from commercial sources and used as received. Carbazole (>95%), *N*-bromosuccinimide (NBS, >99%), potassium permanganate (≥99.0%), 4-formylphenylboronic acid (95%), and *o*-dichlorobenzene were purchased from Sigma–Aldrich. Tetrakis(triphenylphosphine)palladium(0) (99%) and 4-aminophenylboronic acid pinacol ester were obtained from Acros. Potassium carbonate anhydrous (99%), TP (98%), and PD (97%) were purchased from Alfa Aesar. 1,4-Dioxane was purchased from J. T. Baker.

S2. Characterization

^{1}H and ^{13}C NMR spectra were recorded using an INOVA 500 instrument with DMSO-d_6 and $CDCl_3$ as solvents and tetramethylsilane (TMS) as the external standard. Chemical shifts are provided in parts per million (ppm). FTIR spectra were recorded using a Bruker Tensor 27 FTIR spectrophotometer and the conventional KBr plate method; 32 scans were collected at a resolution of 4 cm^{-1}. Solid state nuclear magnetic resonance (SSNMR) spectra were recorded using a Bruker Avance 400 NMR spectrometer and a Bruker magic-angle-spinning (MAS) probe, running 32,000 scans. Cross-polarization with MAS (CPMAS) was used to acquire ^{13}C NMR spectral data at 75.5 MHz. The CP contact time was 2 ms; ^{1}H decoupling was applied during data acquisition. The decoupling frequency corresponded to 32 kHz. The MAS sample spinning rate was 10 kHz. TGA was performed using a TA Q-50 analyzer under a flow of N_2. The samples were sealed in a Pt cell and heated from 40 to 800 °C at a heating rate of 20 °C min^{-1} under N_2 at a flow rate of 50 mL min^{-1}. PXRD was performed using a Siemens D5000 and monochromated $Cu/K\alpha$ ($\lambda = 0.1542$ nm. The sample was spread in a thin layer on the square recess of an XRD sample holder. The BET surface areas and porosimetry measurements of the prepared samples (ca. 20–100 mg) were performed using a Micromeritics ASAP 2020 Surface Area and Porosity analyzer. Nitrogen isotherms were generated through incremental exposure to ultrahigh-purity N_2 (up to ca. 1 atm) in a liquid N_2 (77 K) bath. FE-SEM was conducted using a JEOL JSM-7610F scanning electron

microscope. Samples were subjected to Pt sputtering for 100 s prior to observation. TEM was performed using a JEOL-2100 scanning electron microscope, operated at 200 kV. Molecular modeling was performed using Reflex, a software package for crystal determination from XRD patterns. Unit cell dimensions were first determined manually from the observed XRD peak positions using the coordinates. Samples for UV–Vis and fluorescence spectroscopy were dissolved in suitable organic solvents and placed in a small quartz cell ($0.2 \times 1.0 \times 4.5$ cm^3). UV–Vis absorption spectra were recorded using an F-4500 fluorescence spectrometer. Fluorescence emission spectra were recorded using a LabGuide X350 spectrometer. Lifetimes of samples were measured using a Horiba Fluorolog-3 spectrofluorometer equipped with a 365 nm nanoLED for excitation and a S2 FluoroHub R-928 detector. PLQY were recorded on the HORIBA Fluorolog-3 Photon Counting Spectrofluorometer System with Quanta-φ 6-inch integrating sphere.

S3. Synthetic Procedures

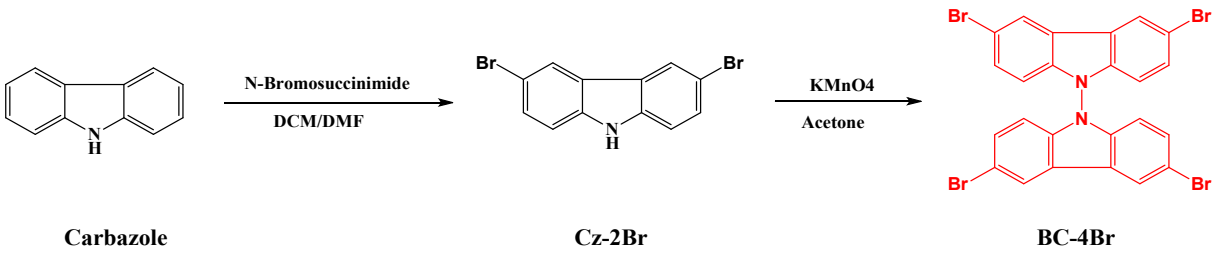

Carbazole **Cz-2Br** **BC-4Br**

Scheme S1. Synthesis of 3,6-dibromocarbazole (Cz-2Br) and 3,3',6,6'-tetrabromo -9,9'-bicarbazole (BC-4Br).

3,6-Dibromocarbazole (Cz-2Br): Prepared as previously reported with slight modification.[S1] A solution of NBS (10.7 g, 60.0 mmol) in DMF (50 mL) was added slowly to a suspension of carbazole (5.00 g, 30.0 mmol) in DCM (300 mL). The mixture was stirred at room temperature overnight. The solution was washed with water (3 × 150 mL); the organic phase was separated and the solvent was evaporated. The solid residue was washed with DCM, then dried under vacuum to yield Cz-2Br (7.7 g, 82%). ^{1}H NMR (500 MHz, DMSO) δ (ppm): 11.58 (br, 1H, NH), 8.41 (s, 2H), 7.52 (d, J = 8.5 Hz, 2 H), 7.42 (d, J = 2 Hz, 2H). ^{13}C NMR (125 MHz, DMSO) δ (ppm): 139.42 (CN), 129.42 (CH), 124.34 (CBr), 123.47 (CH), 112.97 (CH), 112.32 (C).

3,3′,6,6′-Tetrabromo-9,9′-bicarbazole (BC-4Br): Prepared as previously reported with slight modification.[S1] $KMnO_4$ (2.92 g, 90.0 mmol) was added to a solution of Cz-2Br (2.00 g, 30.0 mmol) in acetone (40 mL) at 50 °C. The solution was then hydrolyzed through the addition of distilled water (100 mL). The mixture was extracted with DCM and the solvent evaporated. The residue was washed with MeOH to yield CB-4Br (6.92 g, 71%). ^{1}H NMR (500 MHz, $CDCl_3$) δ (ppm): 8.27 (d, 4H), 7.47 (dd, J = 1.8, 8.5 Hz, 4H), 6.75 (d, J = 8.5 Hz, 4H). ^{13}C NMR (125 MHz, $CDCl_3$) δ (ppm): 139.31 (CN), 131.19 (CH), 124.81 (CH), 123.30 (CBr), 115.41 (C), 110.59 (CH).

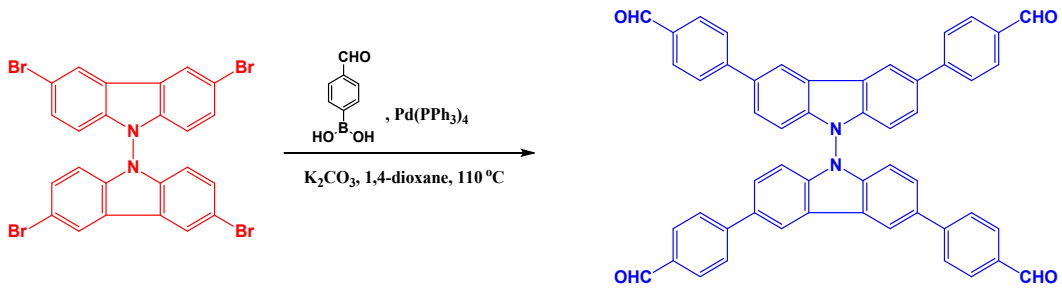

BC-4Br BCTB-4CHO

Scheme S2. Synthesis of 4,4',4",4'"-([9,9'-bicarbazole]-3,3',6,6'-tetrayl)tetrabenz-aldehyde (BCTB-4CHO).

4,4′,4′′,4′′′-([9,9′-Bicarbazole]-3,3′,6,6′-tetrayl)tetrabenzaldehyde (BCTB-4CHO): BC-4Br (1.00 g, 1.54 mmol), 4-formylphenylboronic acid (1.85 g, 12.3 mmol), $Pd(PPh_3)_4$ (90.0 mg, 0.0780 mmol), and K_2CO_3 (2.13 g, 15.4 mmol) were added in a two-neck flask and subjected to a vacuum for 15 min. Dioxane (50 mL) and H_2O (8 mL) were added and then the mixture was heated at 100 °C for 48 h. The solution was poured into a stirred beaker filled with ice cubes and H_2O. The solid was separated through suction filtration, placed in a

beaker, and treated with a little MeOH; the mixture was heated until it boiled, and then the solution was sonicated for 15 min. The undissolved solid was separated through suction filtration, placed in a beaker, and treated with a small amount of DCM; heated until it boiled, followed by sonication for 15 min. After suction filtering, the undissolved solid was dried in an oven for 24 h to give a grey solid (Yield, 90%). ^{1}H NMR (DMSO-d_6, 25 °C, 500 MHz) δ (ppm): 10.06 (d, J = 6 Hz, 4H), 9.06 (s, 4H), 8.015 (d, J = 9 Hz, 16H), 7.761 (d, J = 8.5 Hz, 4H), 6.92 (d, J = 500 Hz, 4H). ^{13}C NMR (DMSO-d_6, 25 °C, 125 MHz) δ (ppm): 193.80, 146.86, 140.58, 135.5, 133.48, 130.85, 128.01, 127.24, 123.36, 121.3, 110.02.

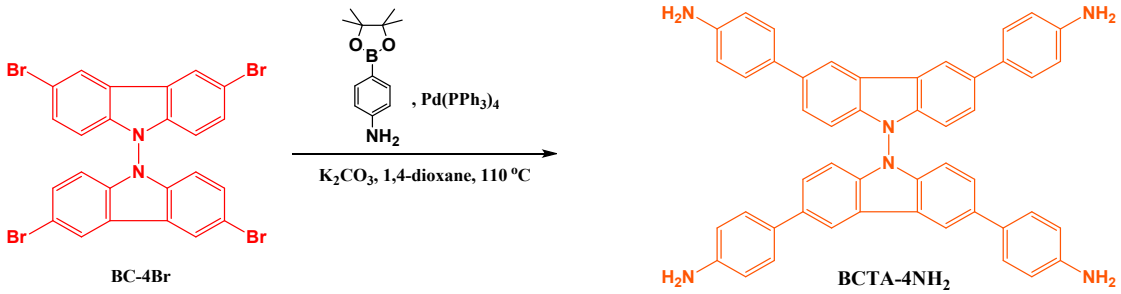

Scheme S3. Synthesis of 4,4',4",4"'-([9,9'-bicarbazole]-3,3',6,6'-tetrayl)tetraaniline (BCTA-4NH_2).

4,4′,4′′,4′′′-([9,9′-Bicarbazole]-3,3′,6,6′-tetrayl)tetraaniline (BCTA-4NH_2): Take a pair of two neck flask, add BC-4Br (1.00 g, 1.54 mmol), 4-aminophenylboronic acid pinacol ester (2.70 g, 12.3 mmol), $Pd(PPh_3)_4$ (90.0 mg, 0.0780 mmol), and K_2CO_3 (2.13 g, 15.4 mmol) were added in a two-neck flask and subjected to a vacuum for 15 min. Dioxane (50 mL) and H_2O (8 mL) were added and then the mixture was heated at 100 °C for 48 h. The solution was poured into a stirred beaker filled with ice cubes and H_2O. The solid was separated

through suction filtration. The crude product was purified chromatographically through (SiO_2; hexane/EtOAc, 3:1) to give BCTA-4NH_2 (Yield, 85%). ^{1}H NMR (DMSO-d_6, 25 °C, 500 MHz) δ (ppm): 8.63 (s, 4H), 7.56 (s, 4H), 7.50 (s, 8H), 6.86 (s, 4H), 6.70 (d, J =10 Hz, 8H), 5.18 (s, 8H). ^{13}C NMR (DMSO-d_6, 25 °C, 125 MHz) δ (ppm): 149.14, 139.72, 135.8, 129.3, 128.52, 125.95, 123.63, 119.06, 115.32, 109.85.

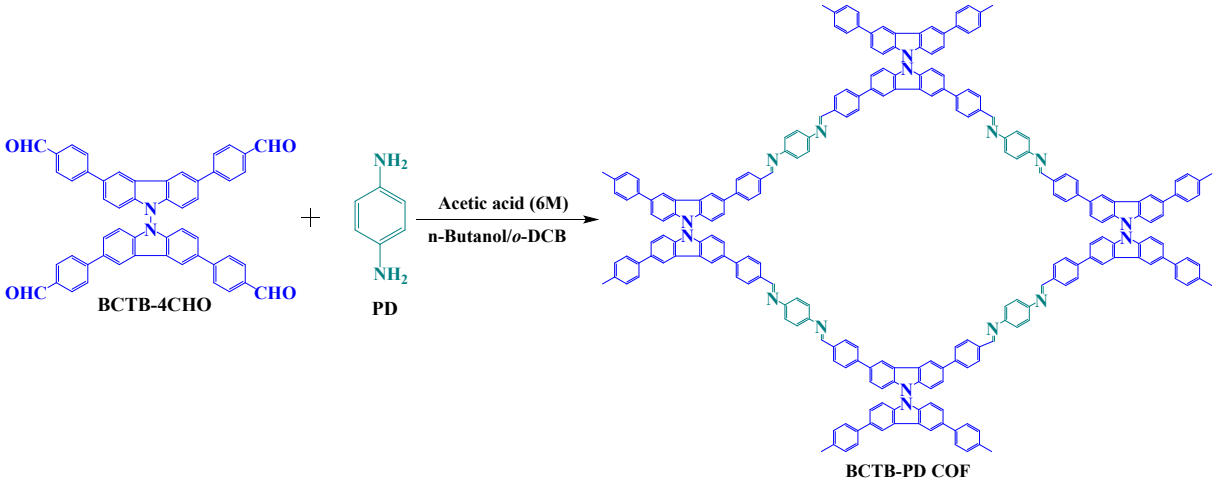

Scheme S4. Synthesis of BCTB-PD COF.

BCTB-PD COF: A solution of BCTB-4CHO (70.0 mg, 0.0934 mmol) and PD (20.2 mg, 0.187 mmol) in *n*-butanol (2.5 mL) and *o*-dichlorobenzene (2.5 mL) containing acetic acid (6 M, 0.5 mL) was degassed in a 25-mL Schlenk storage tube using three freeze/pump/thaw cycles. The tube was sealed off by flame and heated at 120 °C for 3 days. After cooling to room temperature, the tube was opened and the precipitate was filtered off and washed (once with DMF, three times each with THF and acetone). The solid was dried under vacuum at 120 °C overnight to afford the BCTB-PD COF as a brown powder.

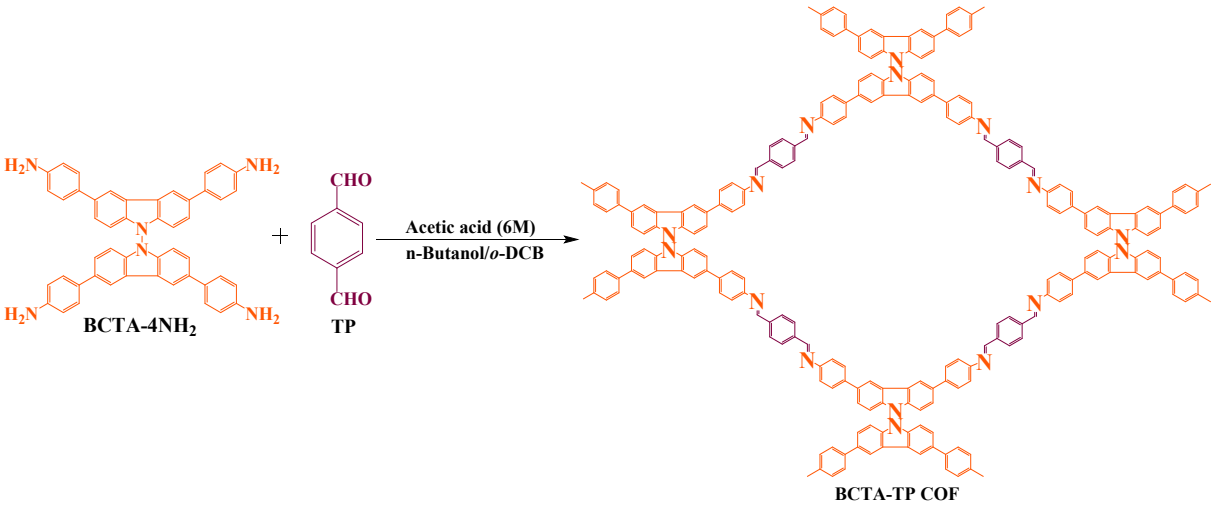

Scheme S5. Synthesis of BCTA-TP COF.

BCTA-TP COF: A solution of BCTA-4NH_2 (70.0 mg, 0.100 mmol) and TP (27.0 mg, 0.201 mmol) in *n*-butanol (2.5 mL) and *o*-dichlorobenzene (2.5 mL) containing acetic acid (6 M, 0.5 mL) was degassed in a 25-mL Schlenk storage tube using three freeze/pump/thaw cycles. The tube was sealed off by flame and heated at 120 °C for 3 days. After cooling to room temperature, the tube was opened and the precipitate was filtered off and washed (once with 1,4-dioxane, three times each with THF and acetone). The solid was dried under vacuum at 120 °C overnight to afford the BCTA-TP COF as a yellow powder.

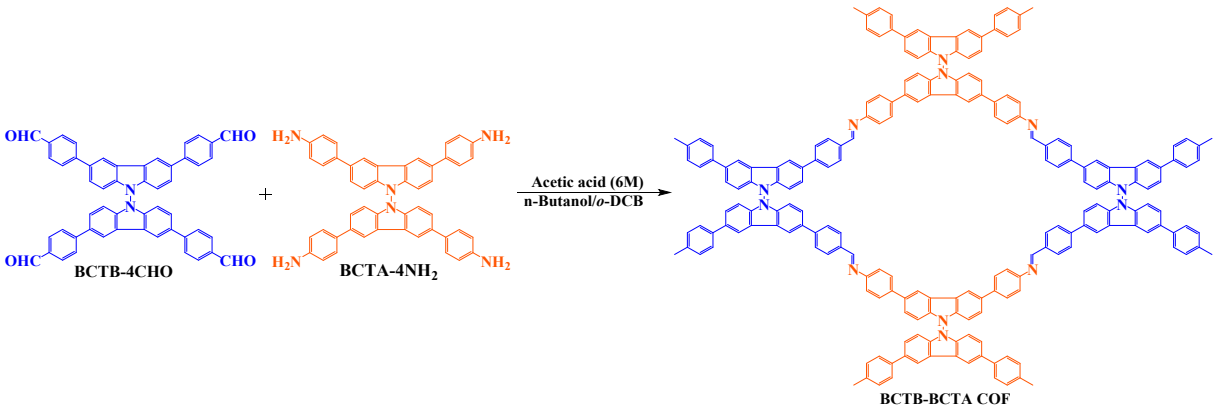

Scheme S6. Synthesis of BCTB-BCTA COF.

BCTB-BCTA COF: A solution of BCTB-4CHO (70 mg, 0.093 mmol) and BCTA-4NH_2 (65.14 mg, 0.093 mmol) in *n*-butanol (2.5 mL) and *o*-dichlorobenzene (2.5 mL) containing acetic acid (6 M, 0.7 mL) was degassed in a 25-mL Schlenk storage tube using three freeze/pump/thaw cycles. The tube was sealed off by flame and heated at 120 °C for 3 days. After cooling to room temperature, the tube was opened and the precipitate was filtered off and washed (one time with DMF, three times each with THF and acetone). The solid was dried under vacuum at 120 °C overnight to afford the BCTB-BCTA COF as a brown powder.

S4. IR Spectral Profiles of Monomers

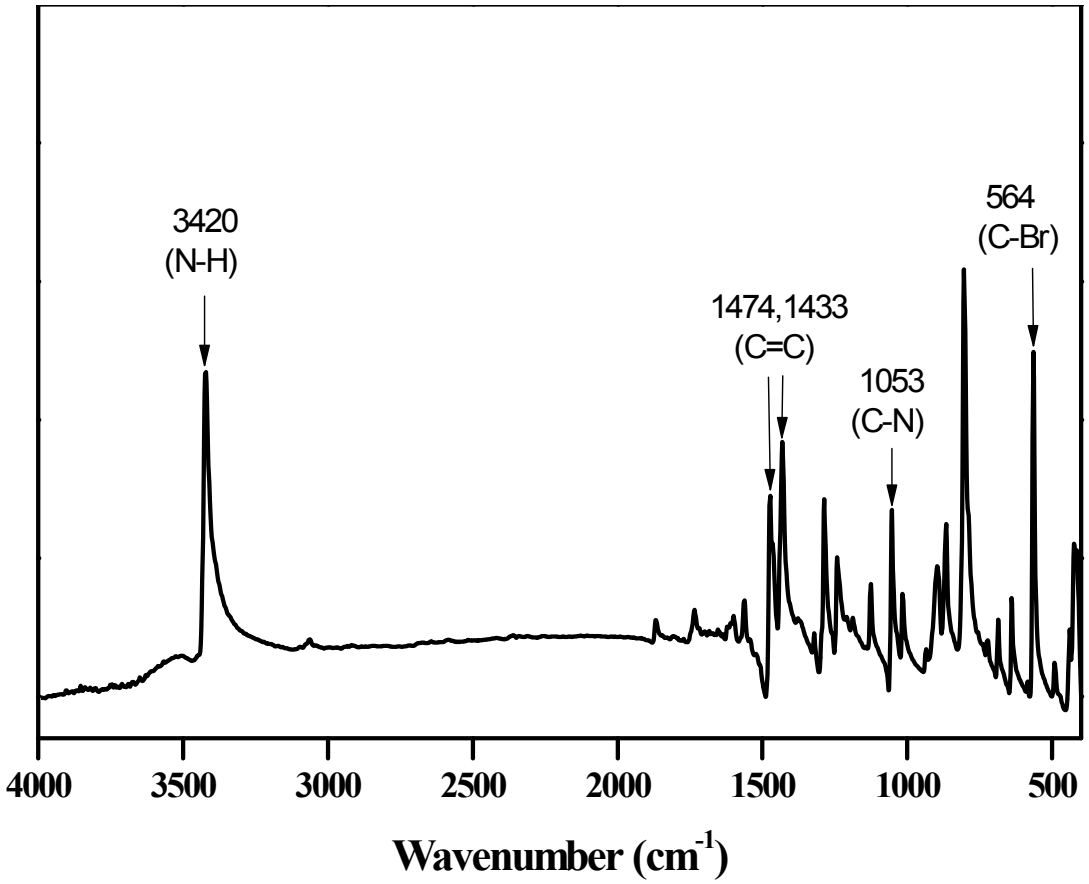

Figure S1. IR spectrum of 3,6-dibromocarbazole (Cz-2Br).

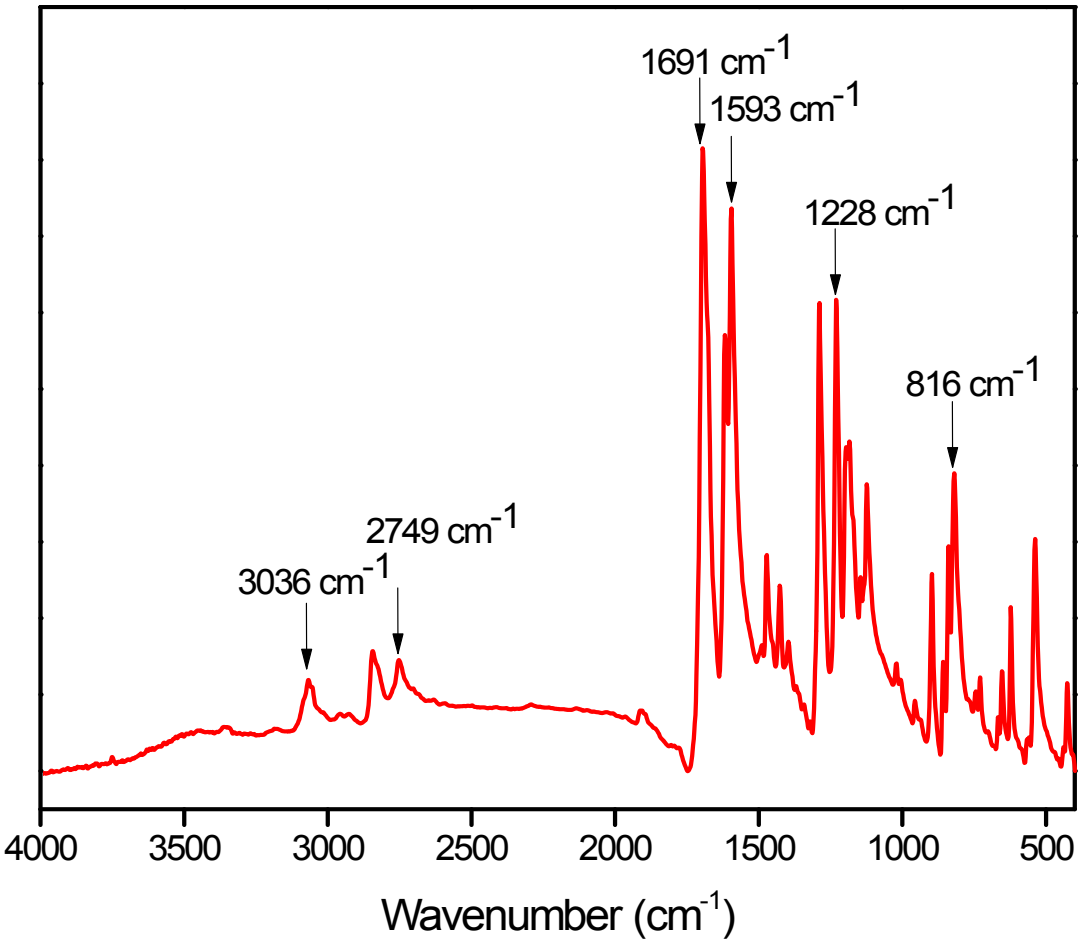

Figure S2. IR spectrum of 3,3'6,6'-tetrabromo-9,9'-bicarbazole (BC-4Br).

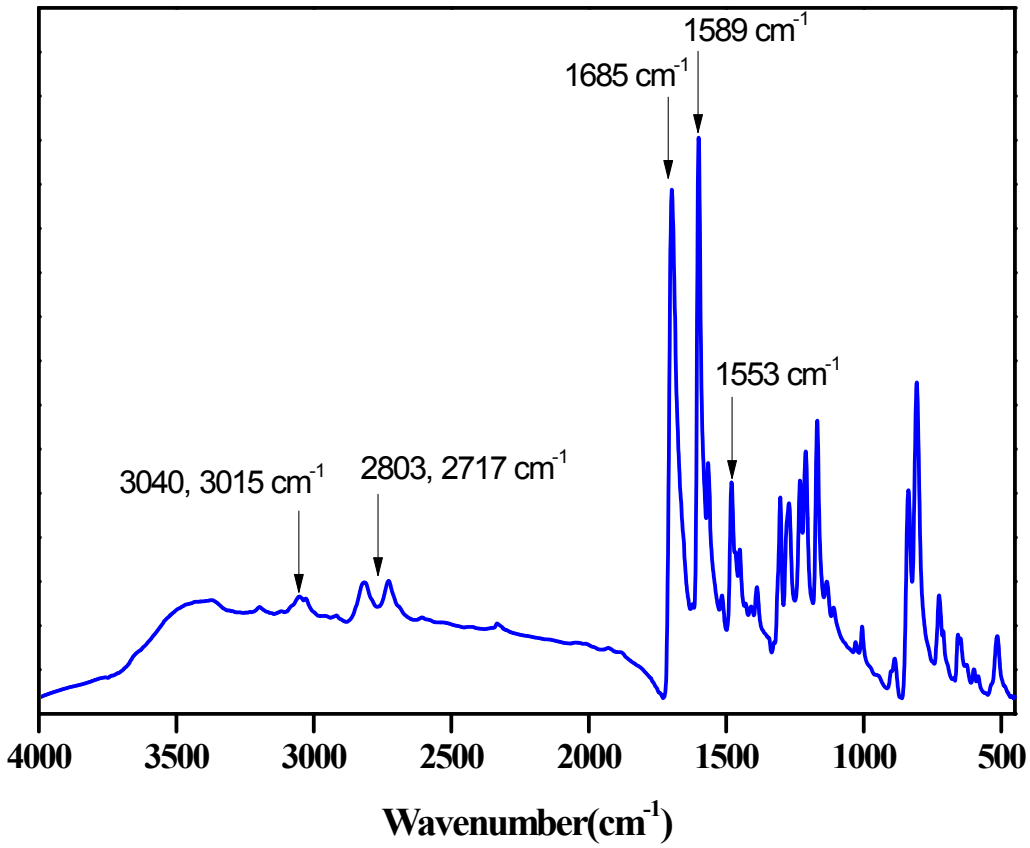

Figure S3. IR spectrum of 4,4',4'',4'''-([9,9'-bicarbazole]-3,3',6,6'-tetrayl)tetrabenzaldehyde (BCTB-4CHO).

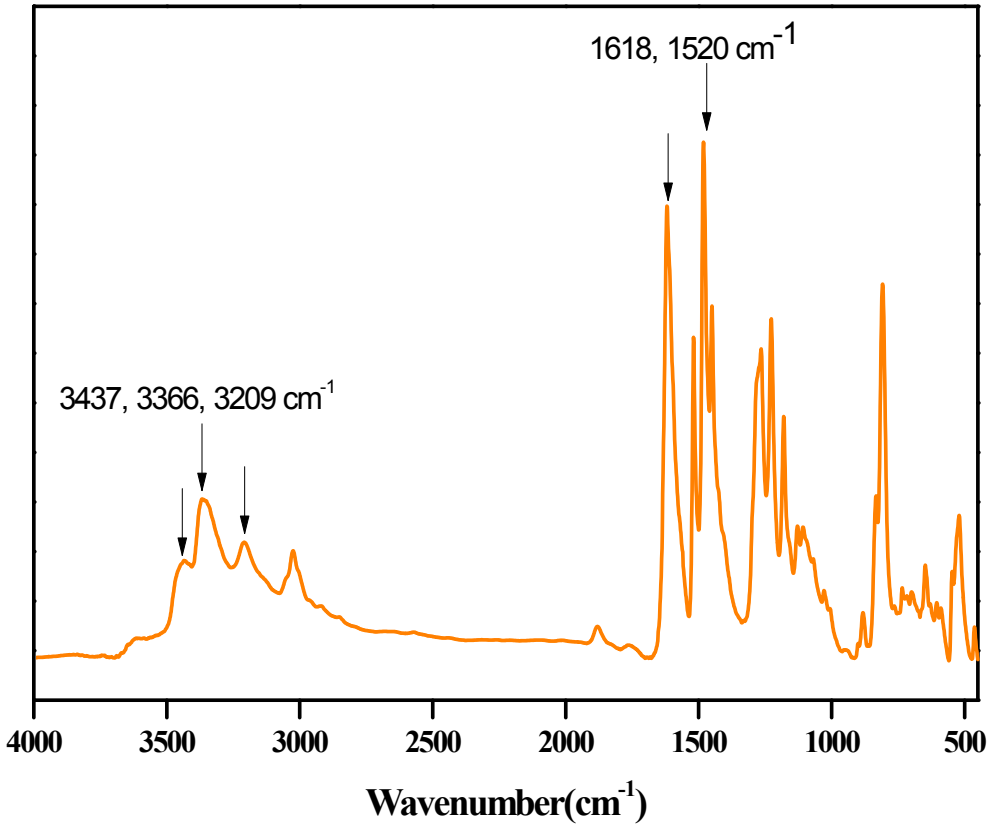

Figure S4. IR spectrum of 4,4',4",4'"-([9,9'-bicarbazole]-3,3',6,6'-tetrayl)tetraaniline (BCTA-$4NH_2$).

S5. NMR Spectral Profiles of Monomers

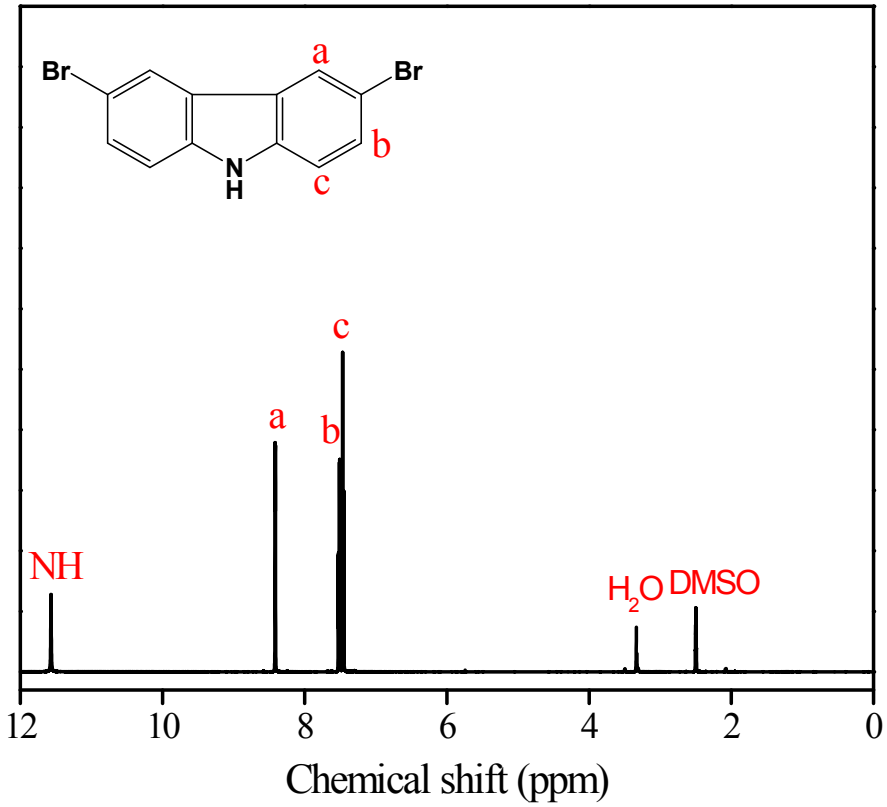

Figure S5. ^{1}H-NMR of 3,6-dibromocarbazole (Cz-2Br).

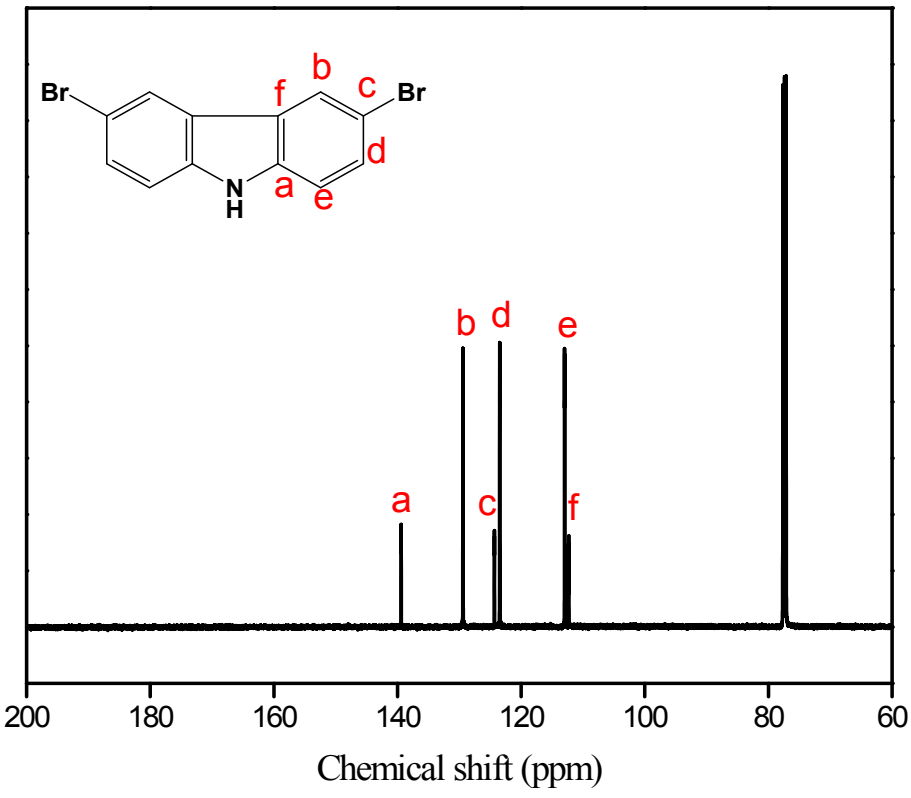

Figure S6. ^{13}C-NMR of 3,6-dibromocarbazole (Cz-2Br).

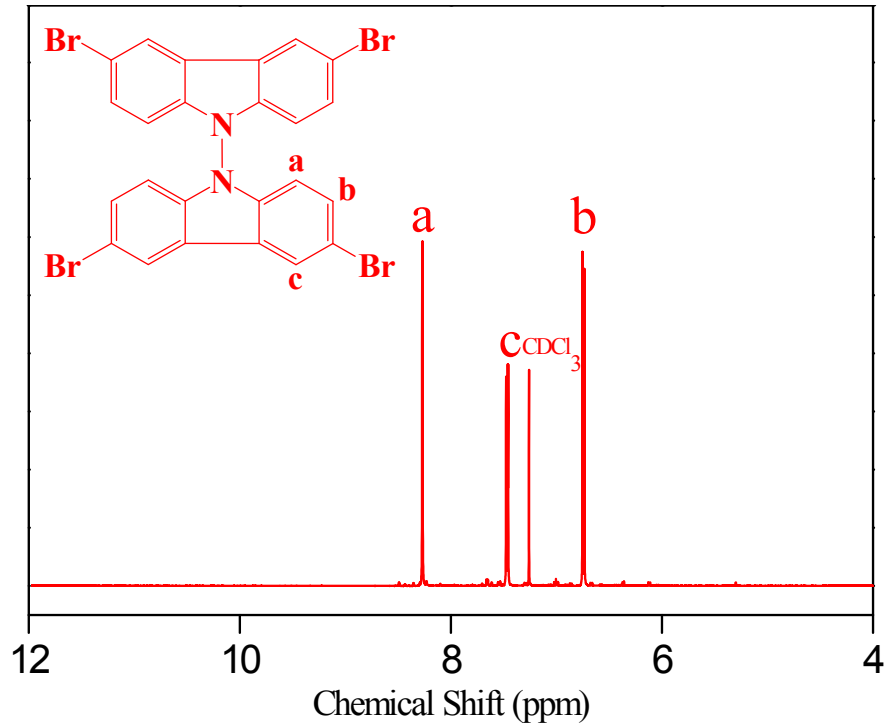

Figure S7. ^{1}H-NMR of 3,3'6,6'-tetrabromo-9,9'-bicarbazole (BC-4Br).

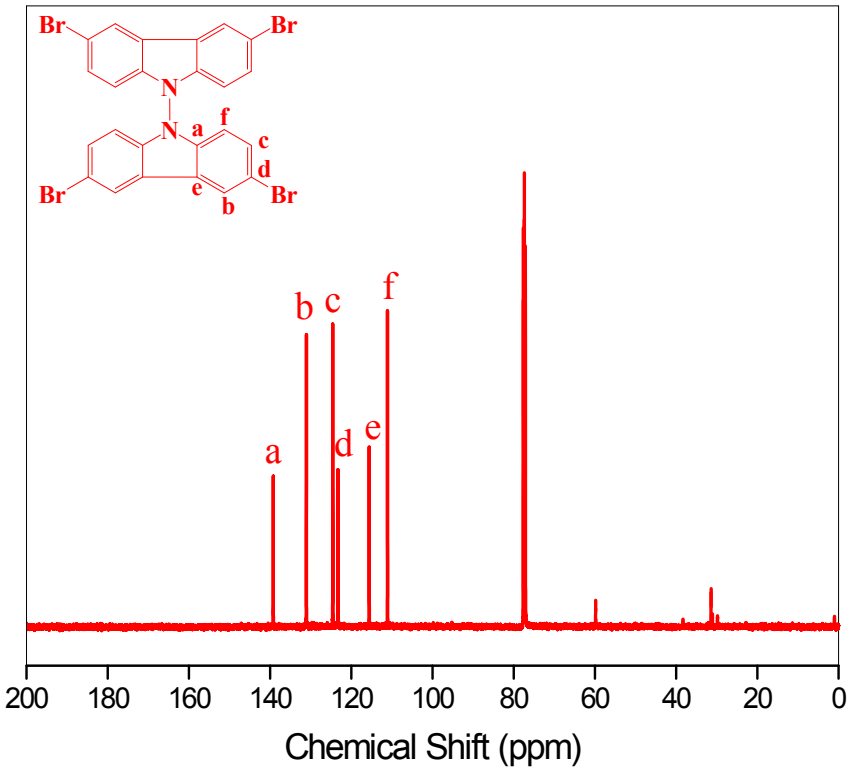

Figure S8. ^{13}C-NMR of 3,3'6,6'-tetrabromo-9,9'-bicarbazole (BC-4Br).

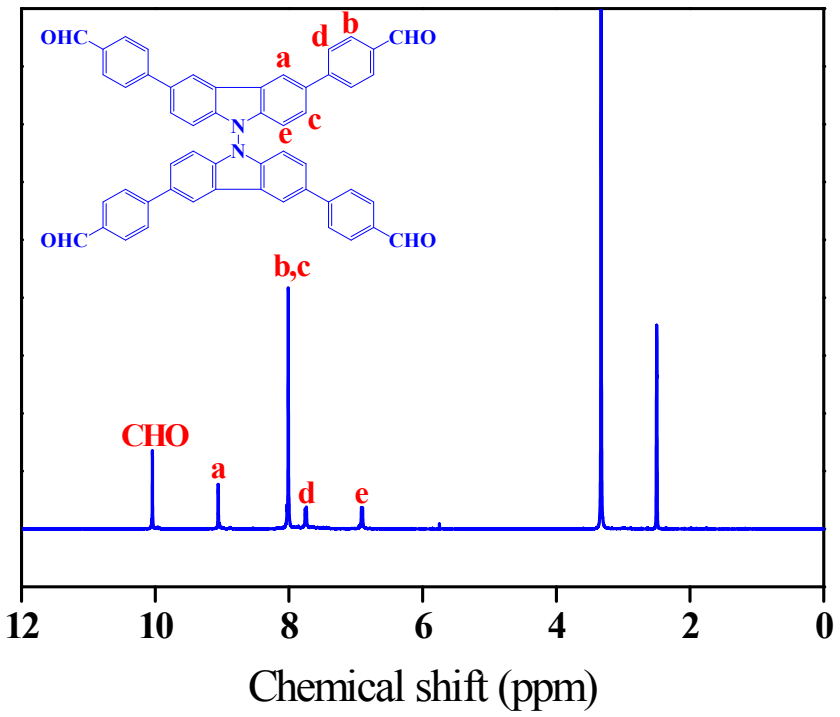

Figure S9. ^{1}H-NMR of 4,4',4",4"'-([9,9'-bicarbazole]-3,3',6,6'-tetrayl)tetrabenzaldehyde (BCTB-4CHO).

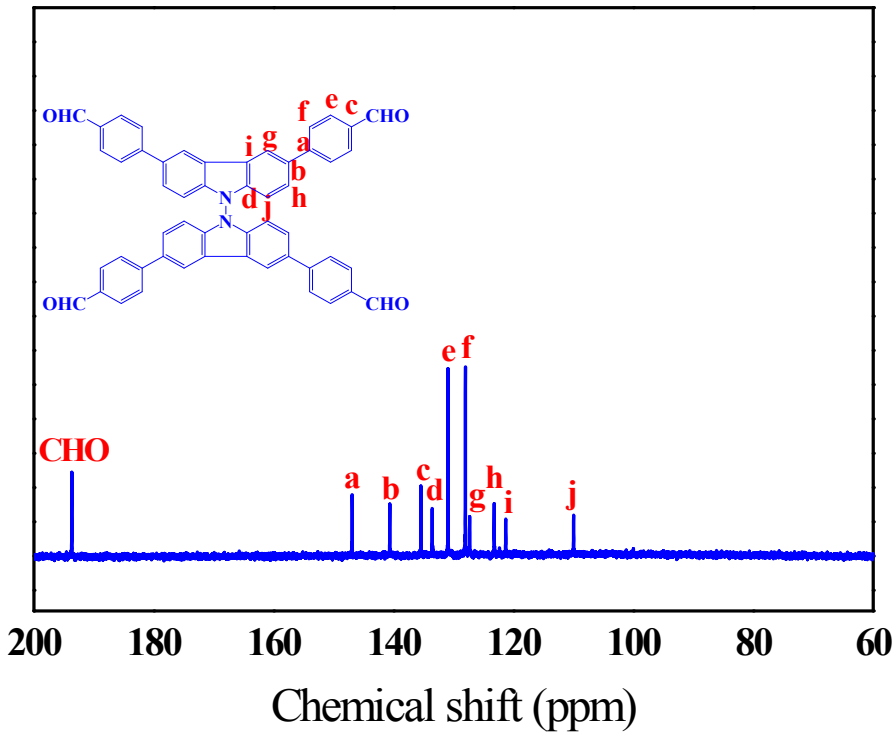

Figure S10. ^{13}C-NMR of 4,4',4",4"'-([9,9'-bicarbazole]-3,3',6,6'-tetrayl)tetrabenzaldehyde (BCTB-4CHO).

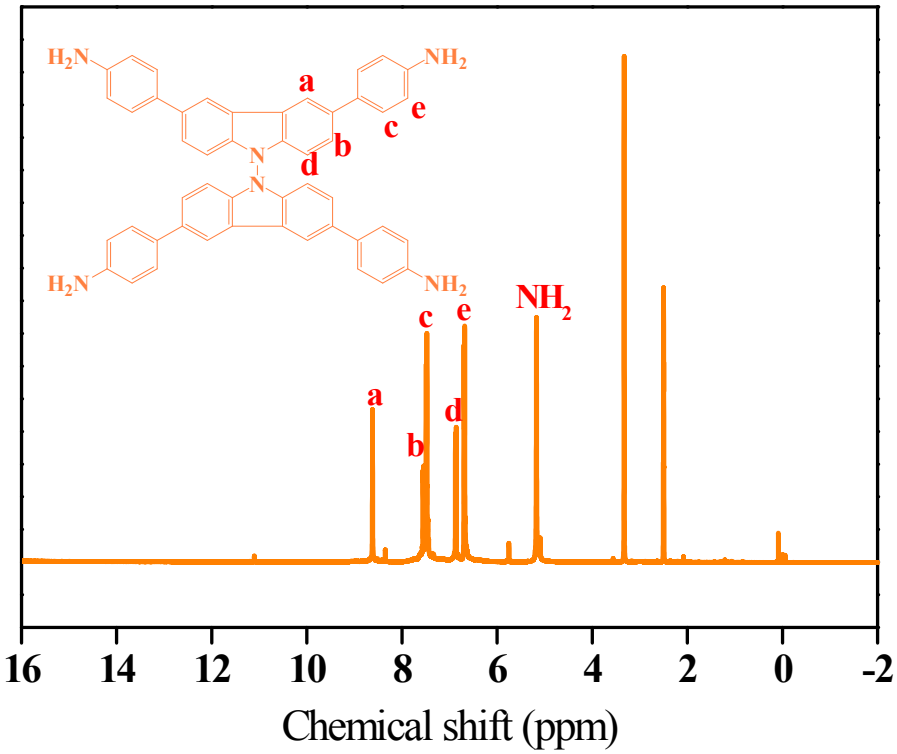

Figure S11. ^{1}H-NMR of 4,4',4",4"'-([9,9'-bicarbazole]-3,3',6,6'-tetrayl)tetraaniline (BCTA-4NH_2).

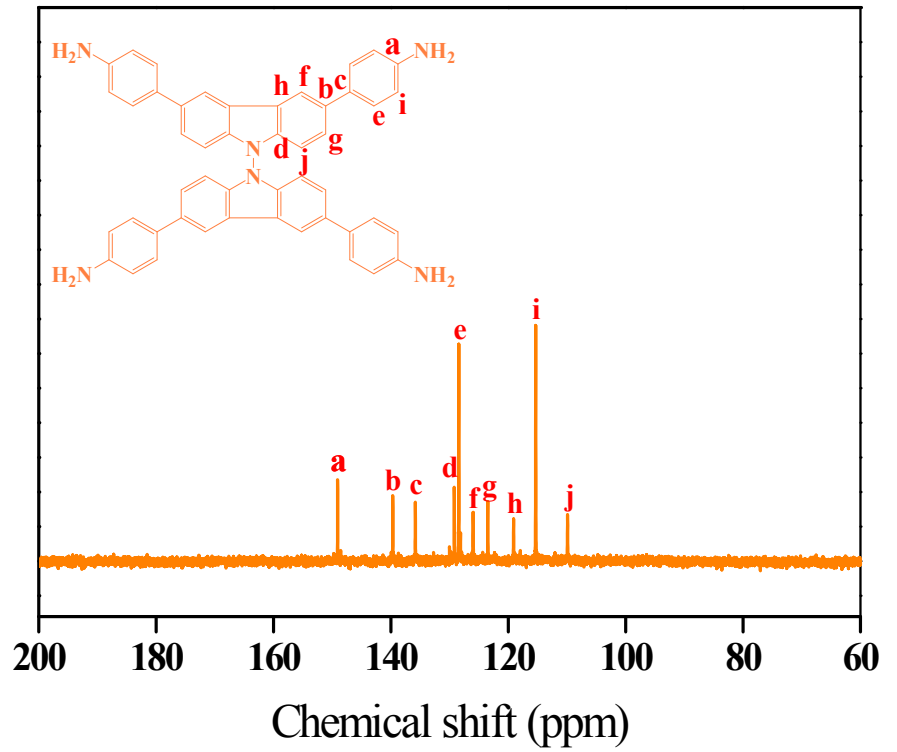

Figure S12. ^{13}C-NMR of 4,4',4",4"'-([9,9'-bicarbazole]-3,3',6,6'-tetrayl)tetraaniline (BCTA-4NH_2).

S6. FTIR Spectral Profiles of Monomers and COFs

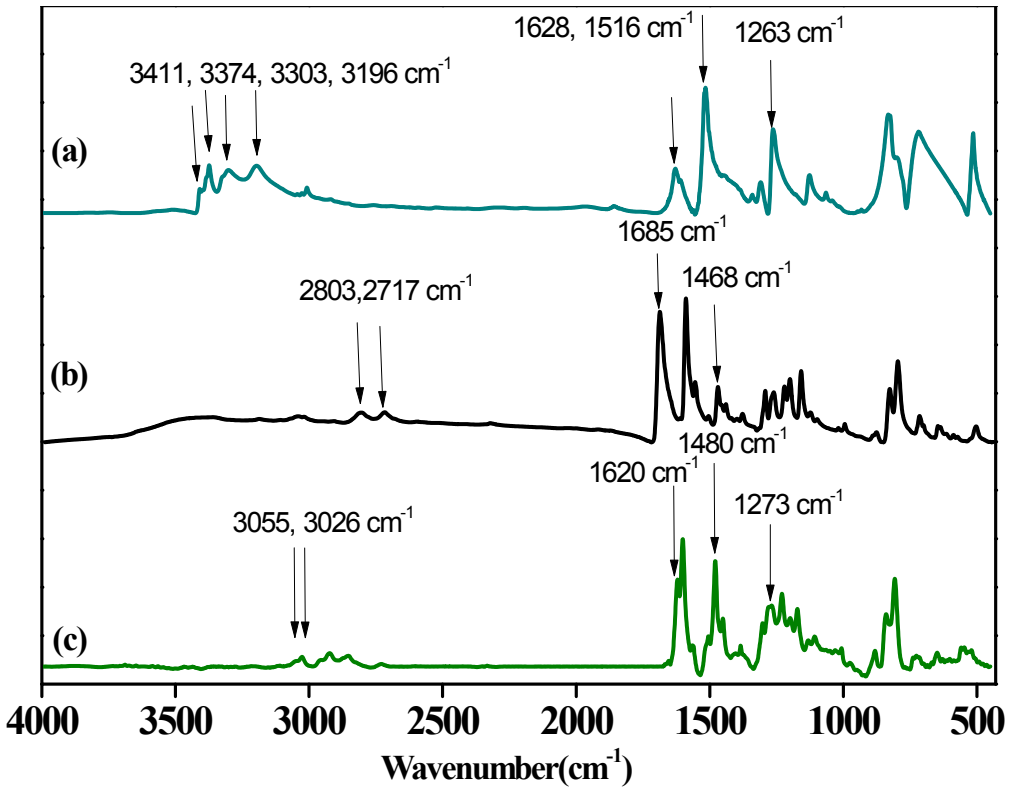

Figure S13. FTIR spectra of (a) PD, (b) BCTB-4CHO, and (c) BCTB-PD COF.

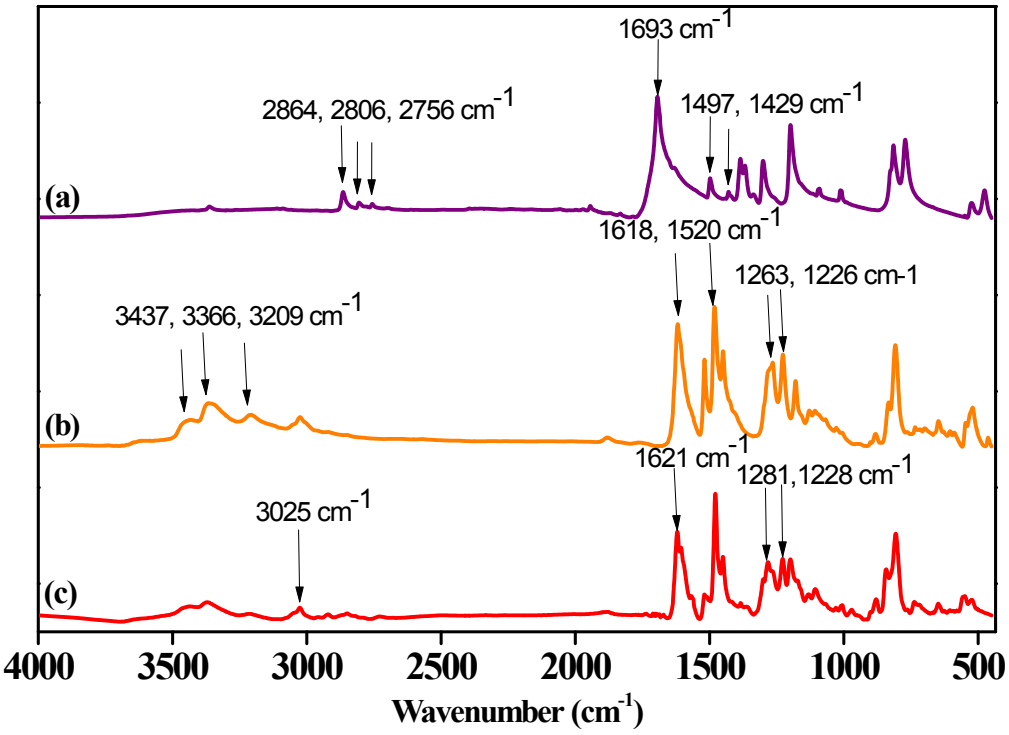

Figure S14. FTIR spectra of (a) TP, (b) BCTA-4NH_2, and (c) BCTA-TP COF.

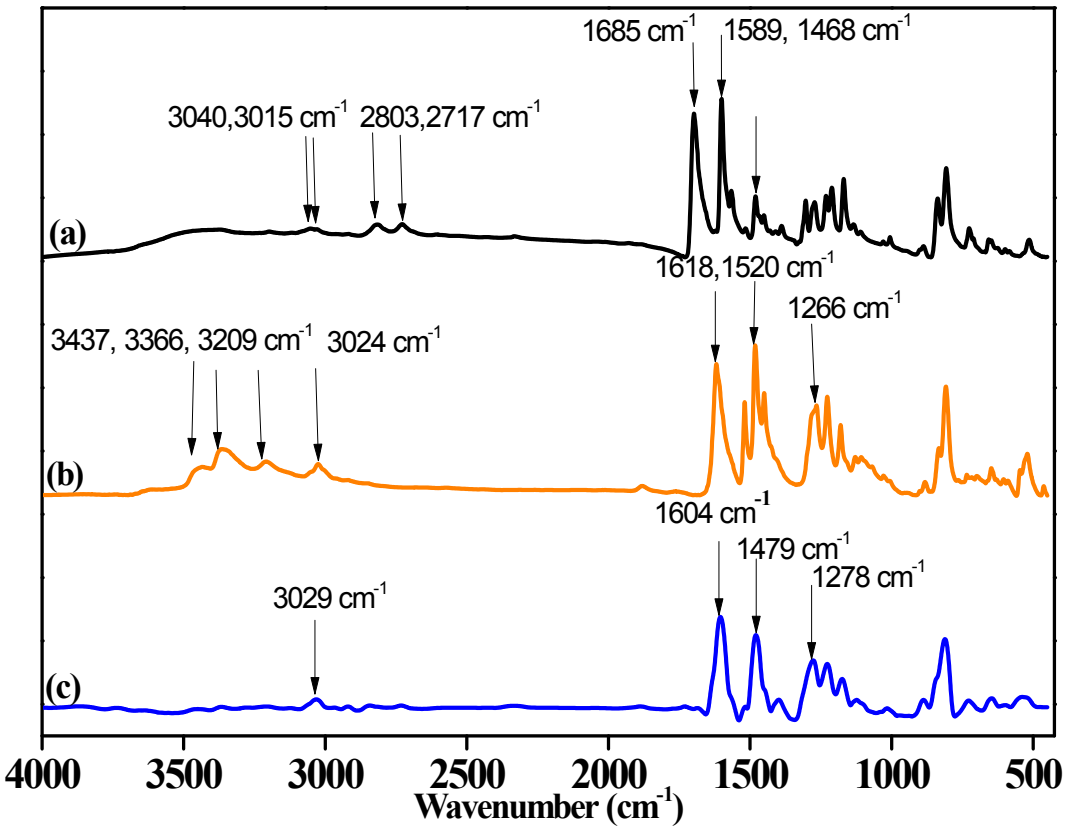

Figure S15. FTIR spectra of (a) BCTB-4CHO, (b) BCTA-4NH_2, and (c) BCTB-BCTA-COF.

S7. Solid-state ^{13}C CP MAS NMR Spectra

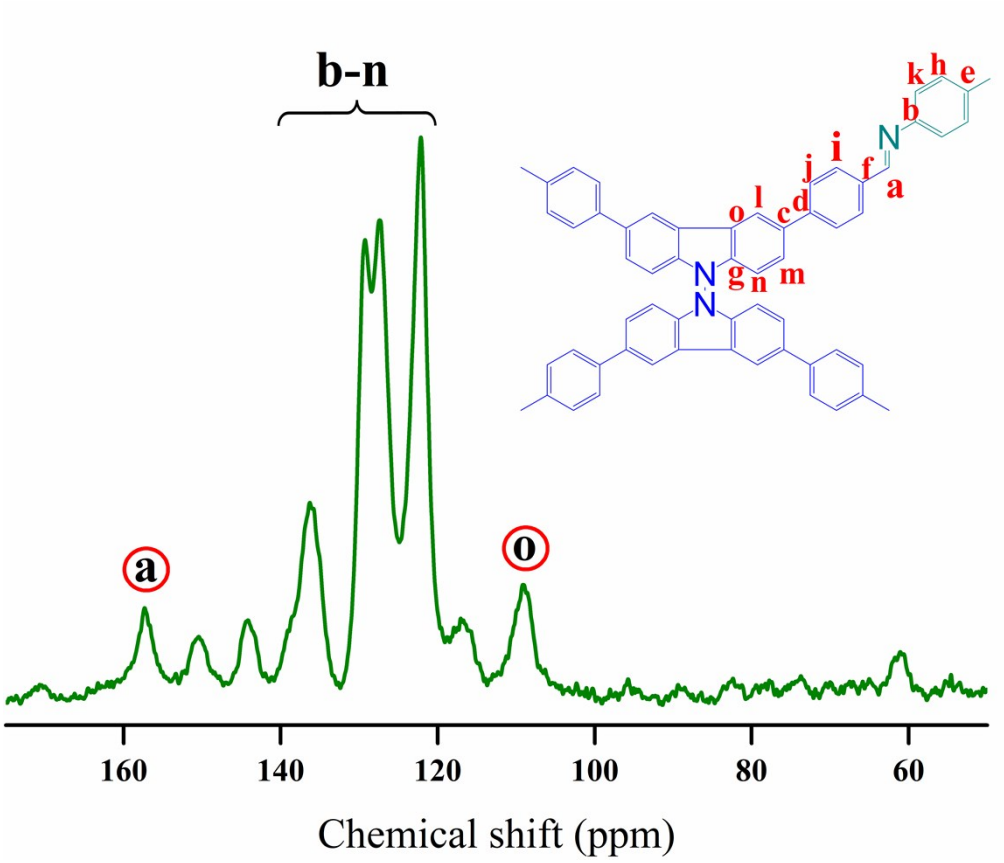

Figure S16. ^{13}C cross-polarization magic angle spinning solid-state NMR of BCTB-PD COF.

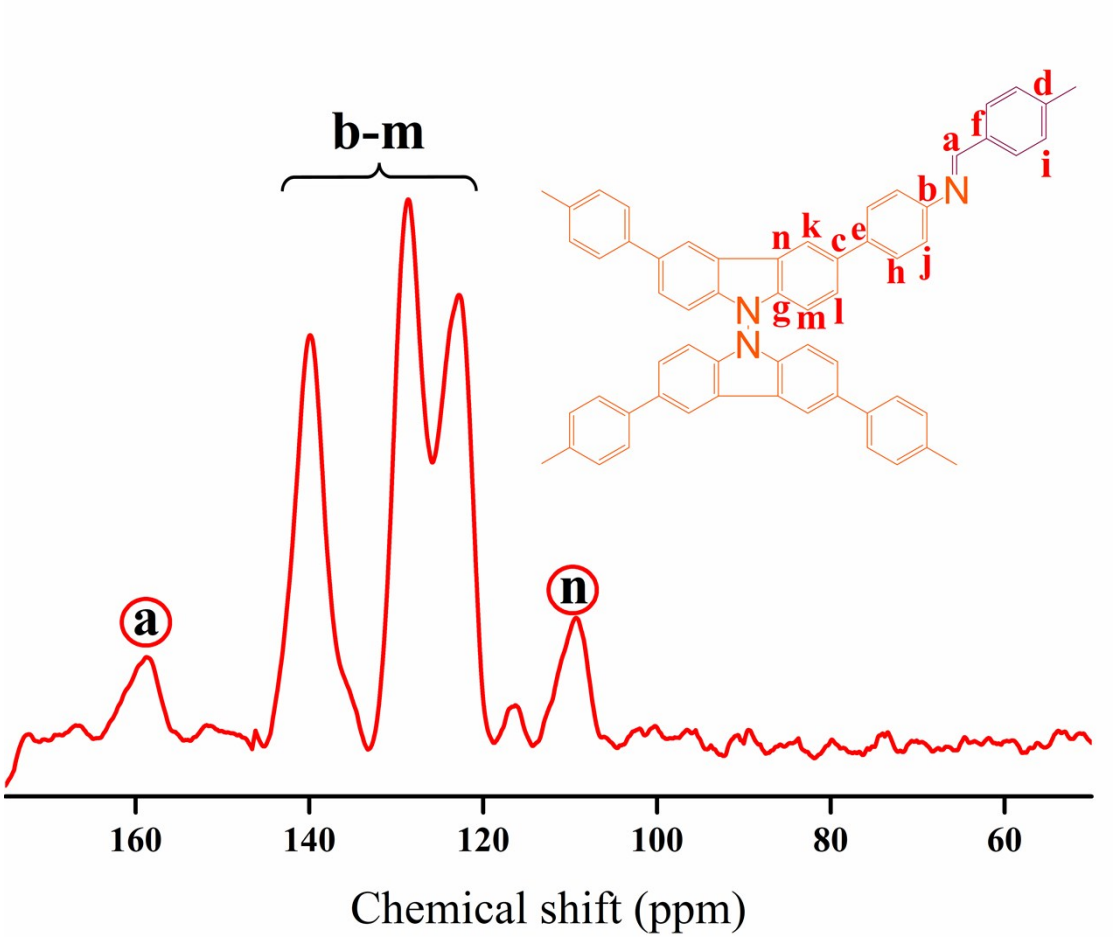

Figure S17. ^{13}C cross-polarization magic angle spinning solid-state NMR of BCTA-TP COF.

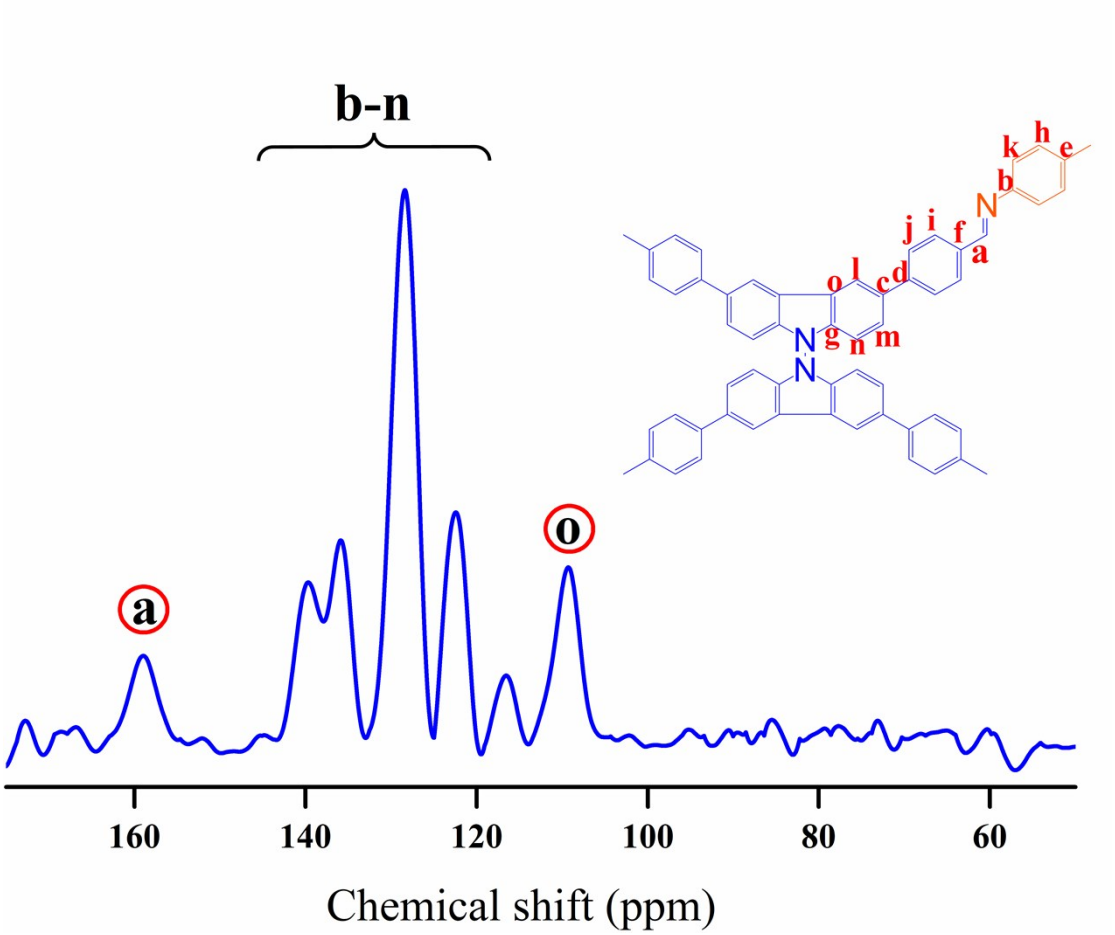

Figure S18. ^{13}C cross-polarization magic angle spinning solid-state NMR of BCTB-BCTA COF.

S8. Thermal Gravimetric Analysis

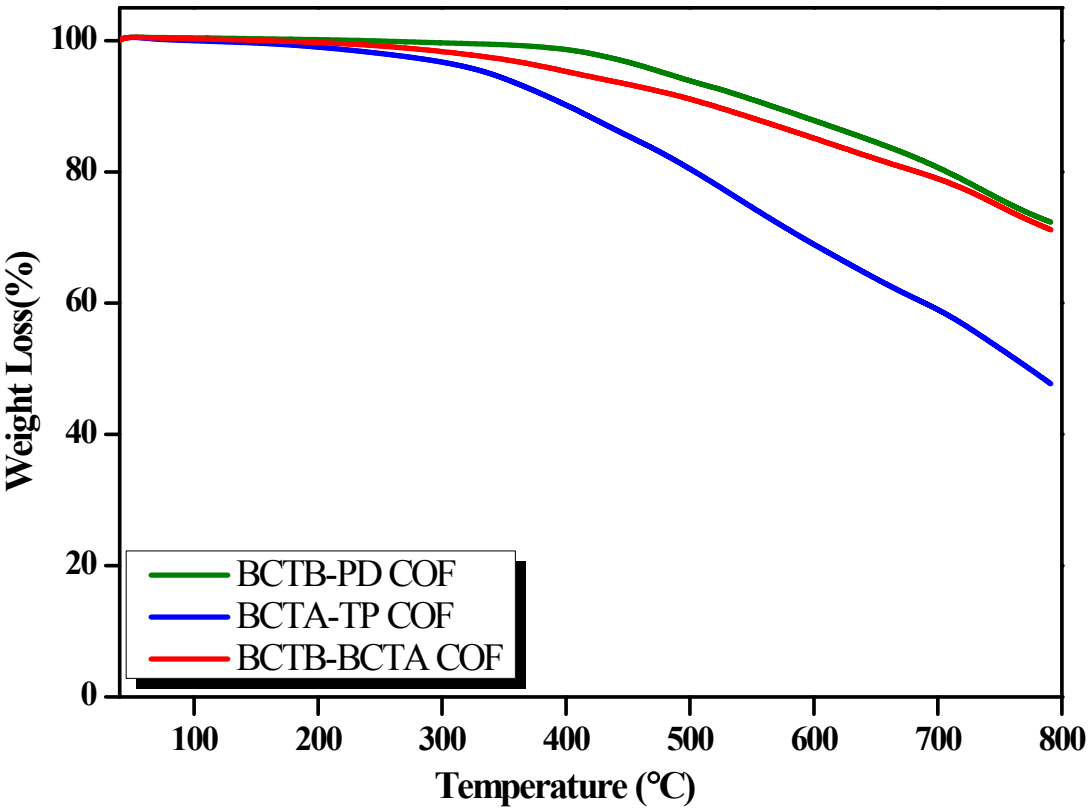

Figure S19. TGA analyses of BCTB-PD, BCTA-TP, and BCTB-BCTA COFs.

Table S1. Values of $T_{d10\%}$, T_{Onset} and Char yield of COFs.

	BCTB-PD	**BCTA-TP**	**BCTB-BCTA**
$T_{d10\%}$ (°C)	566	402	522
T_{Onset} (°C)	550	498	530
Char yield (%)	72	48	71

S9. Transmission Electron Microscopy (TEM)

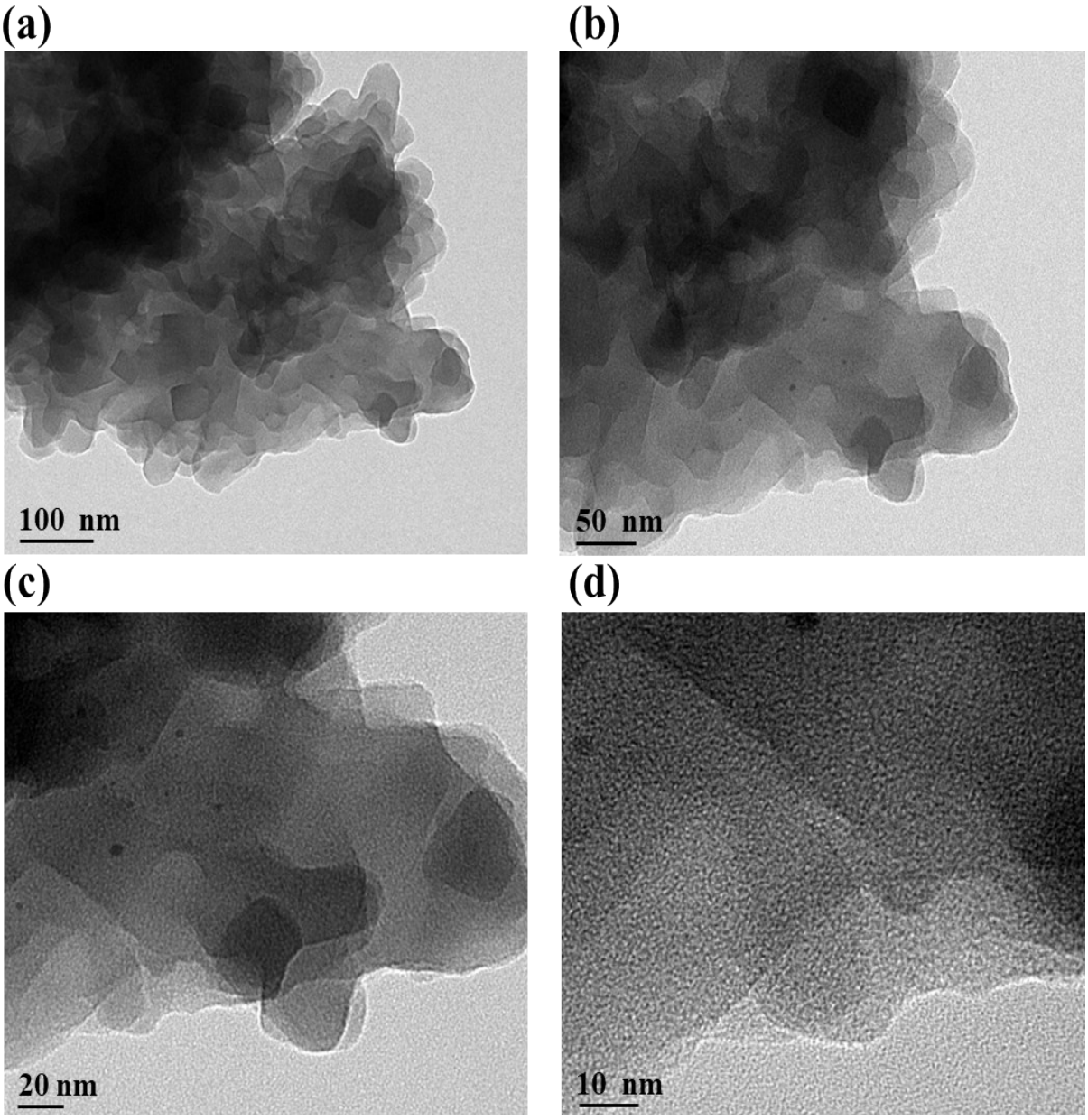

Figure S20. TEM images of the BCTB-PD COF recorded at various magnifications: (a) 100 nm, (b) 50 nm, (c) 20 nm, and (d) 10 nm.

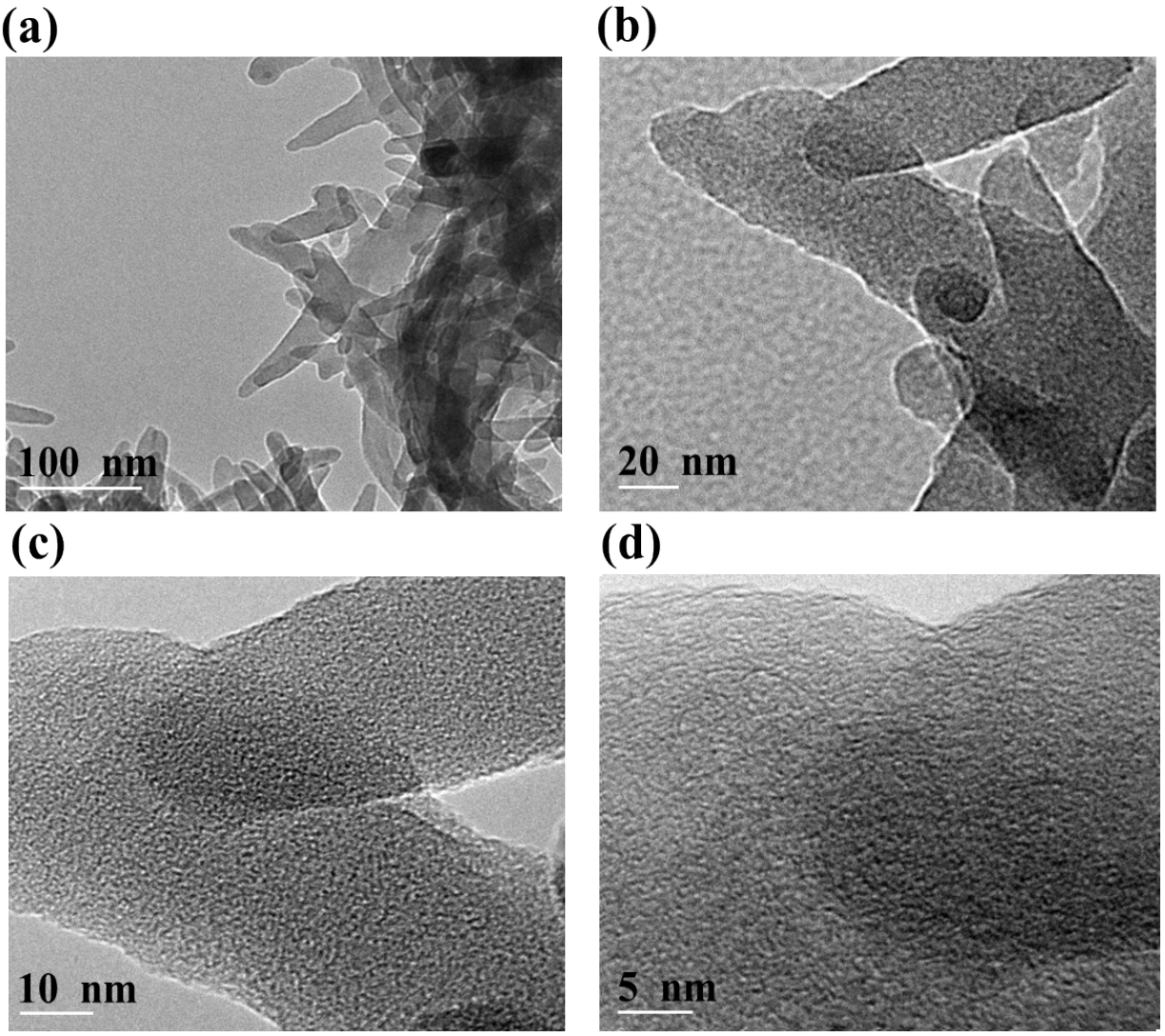

Figure S21. TEM images of the BCTA-TP COF recorded at various magnifications: (a) 100 nm, (b) 20 nm, (c) 10 nm, and (d) 5 nm.

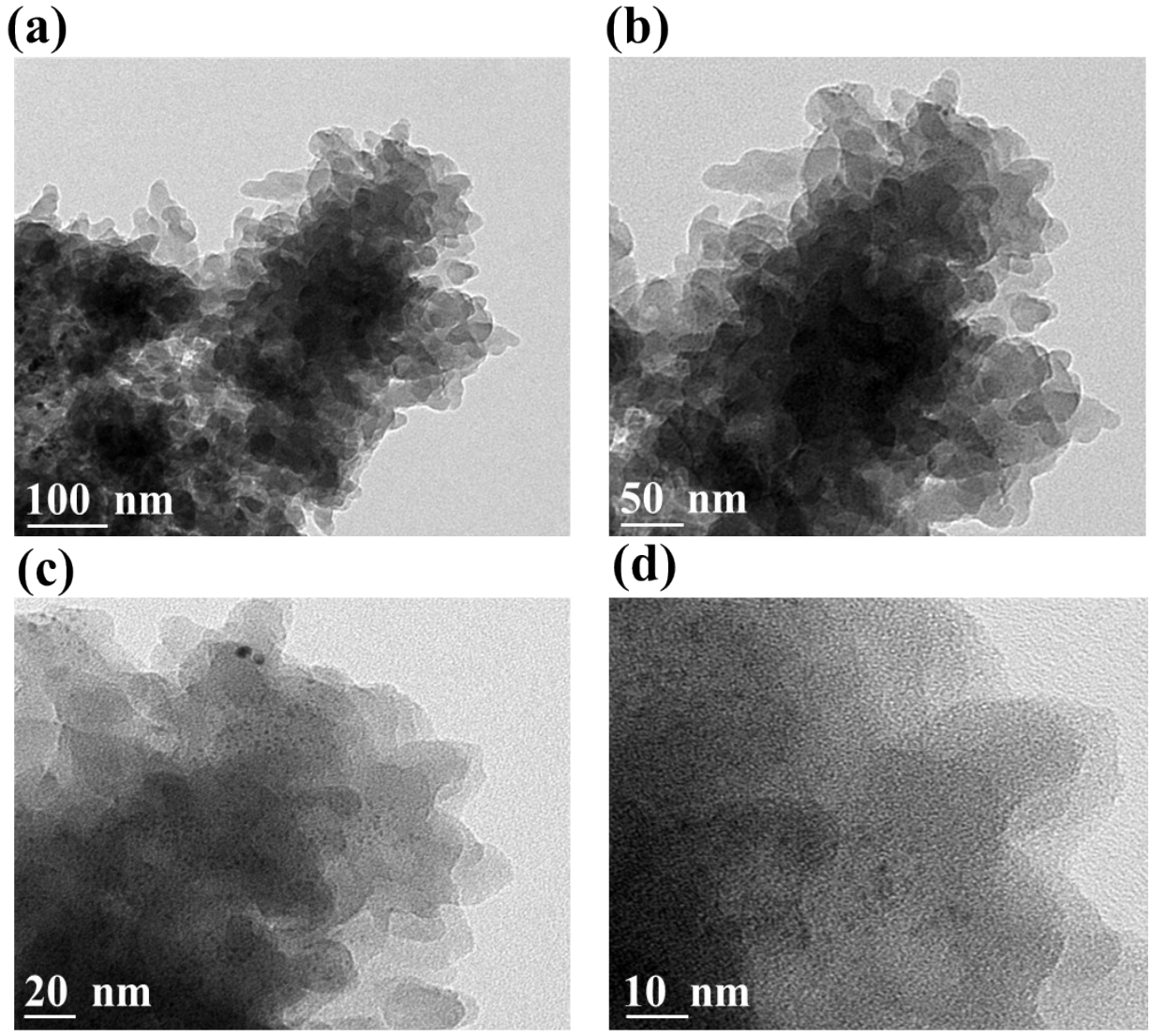

Figure S22. TEM images of the BCTB-BCTA COF recorded at various magnifications: (a) 100 nm, (b) 50 nm, (c) 20 nm, and (d) 10 nm.

S10. Field Emission Scanning Electron Microscopy (FE-SEM)

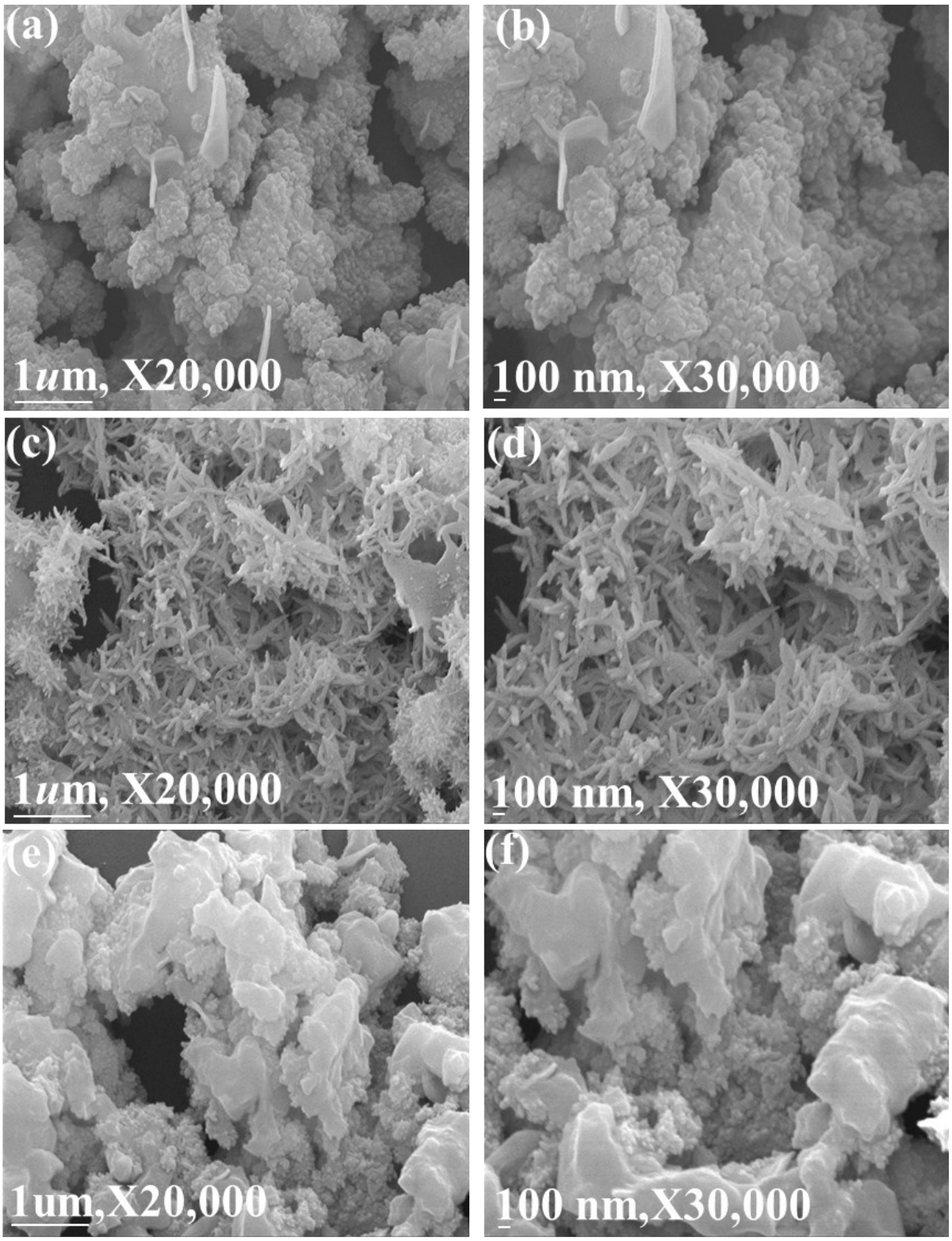

Figure S23. FE-SEM images of the (a, b) BCTB-PD, (c, d) BCTA-TP, and (e, f) BCTB-BCTA COFs, recorded at various magnifications: (a, c, e) 1μm and (b, d, f) 100 nm.

S11. Experimental and Simulation X-ray Diffraction Patterns for COFs Structures

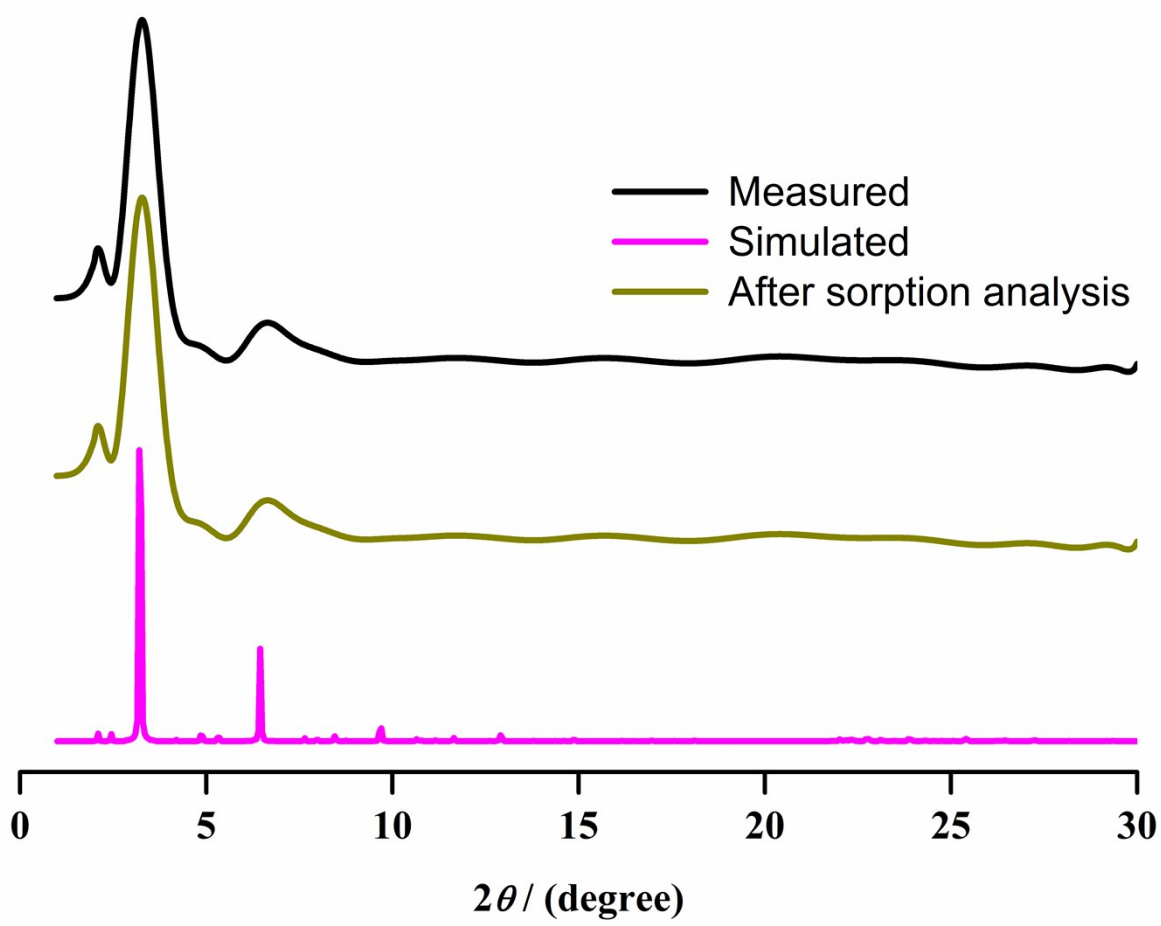

Figure S24. PXRD pattern of as-synthesized BCTB-PD COF (black) and after nitrogen sorption analysis (dark yellow) compared with the simulated PXRD pattern of eclipsed A–A stacking modeling (magenta).

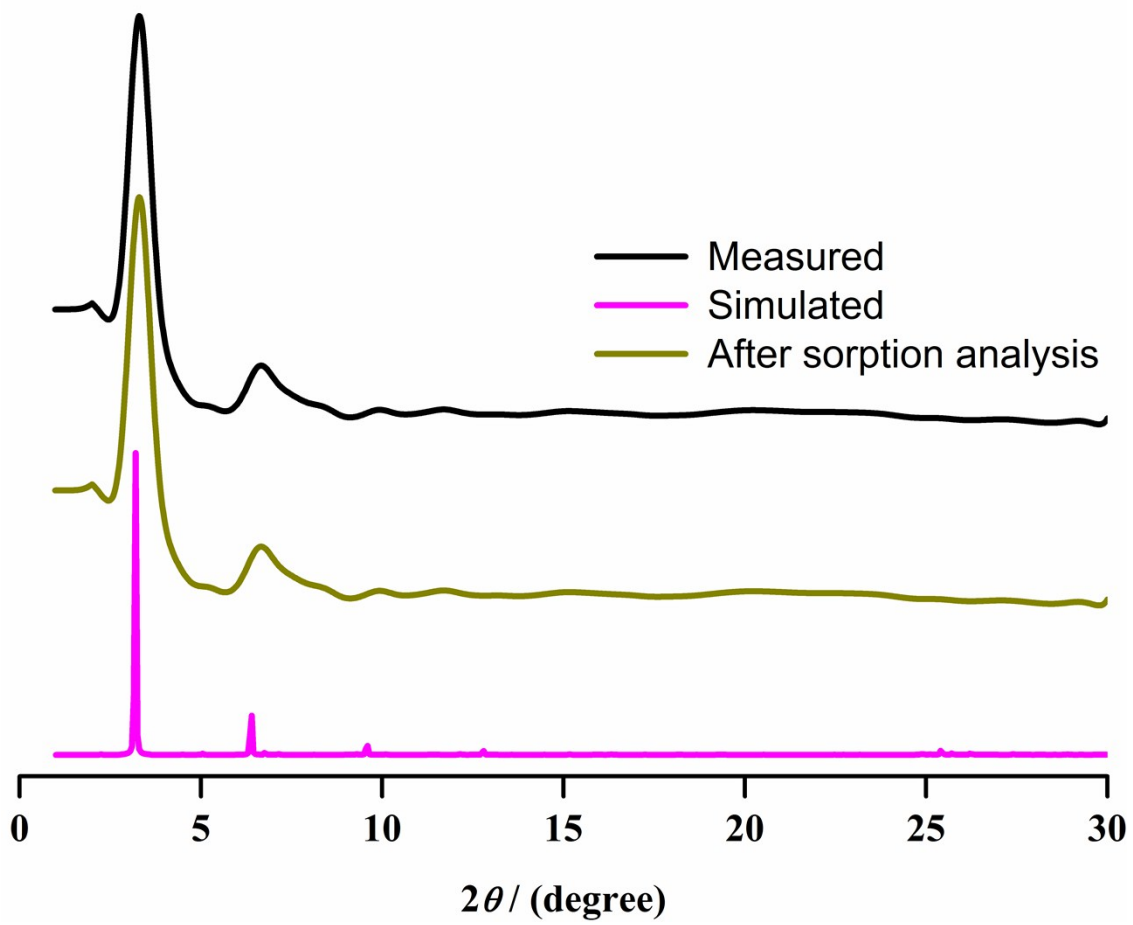

Figure S25. PXRD pattern of as-synthesized BCTA-TP COF (black) and after nitrogen sorption analysis (dark yellow) compared with the simulated PXRD pattern of eclipsed A–A stacking modeling (magenta).

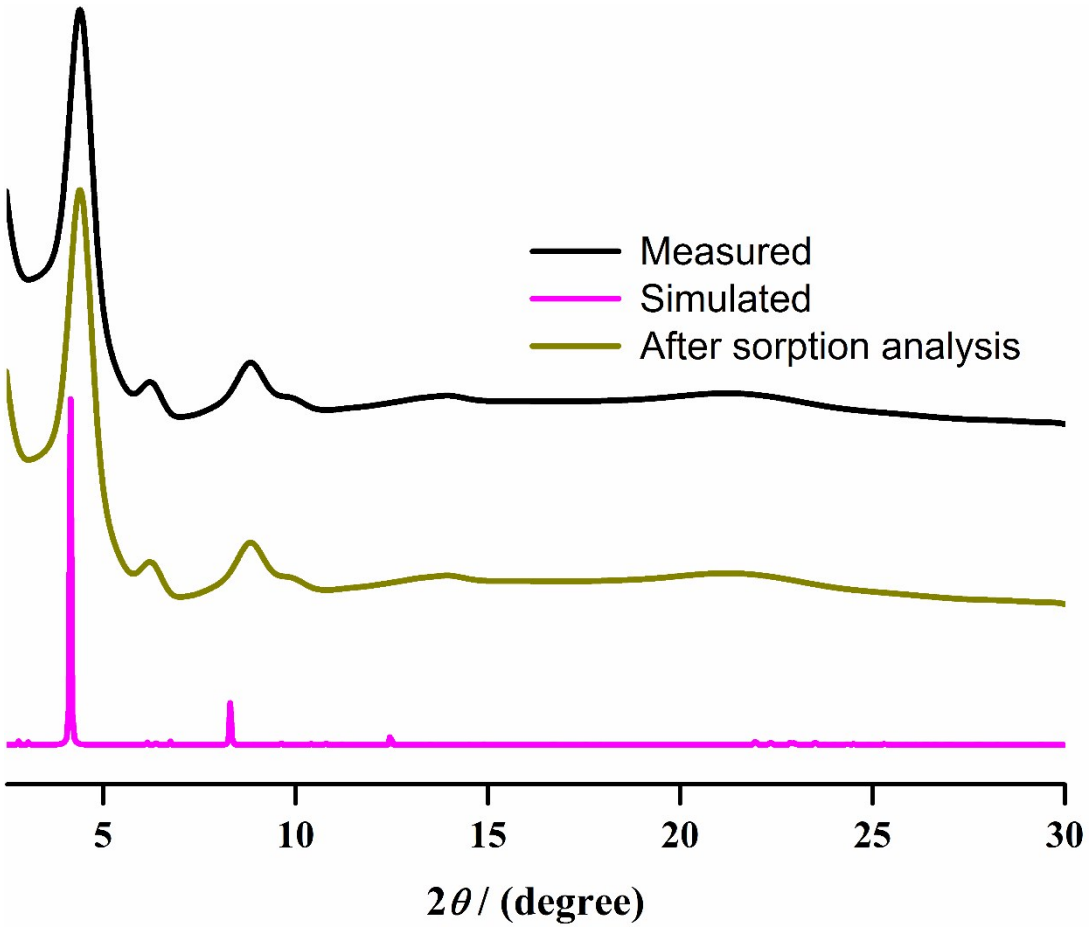

Figure S26. PXRD pattern of as-synthesized BCTB-BCTA COF (black) compared with the simulated PXRD pattern of eclipsed A–A stacking modeling (magenta).

S12. PXRD data and BET parameters

Table S2. PXRD data and BET parameters of the synthesized BCTB-PD, BCTA-TP, and BCTB-BCTA COFs.

COFs	S_{BET} (m^2 g^{-1})	d_{110} (nm)	Pore size (nm)	Interlayer distance (Å)	Pore Volume (cm^3 g^{-1})
BCTB-PD COF	2212	2.73	1.62	3.99	0.28
BCTA-TP COF	645	2.58	1.55	4.05	0.31
BCTB-BCTA COF	1098	1.97	1.10	4.18	0.35

S13. 3D-space Modeling of COFs for two probable structures

Table S3. Views of space models of BCTB-PD COF (a) eclipsed A–A stacking and (b) staggered A–B stacking crystal structure.

(a)	(b)
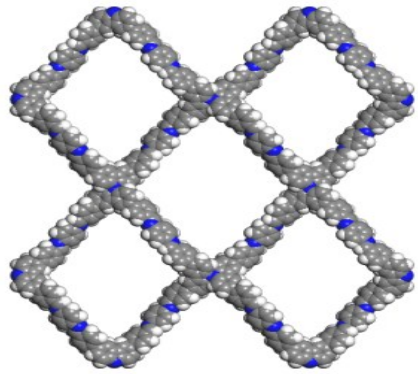	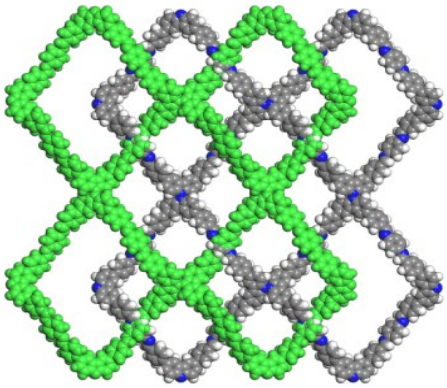
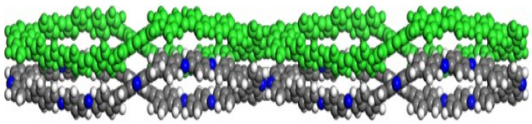	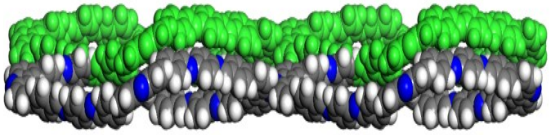

Table S4. Views of space models of BCTA-TP COF (a) eclipsed A–A stacking and (b) staggered A–B stacking structure.

(a)	(b)
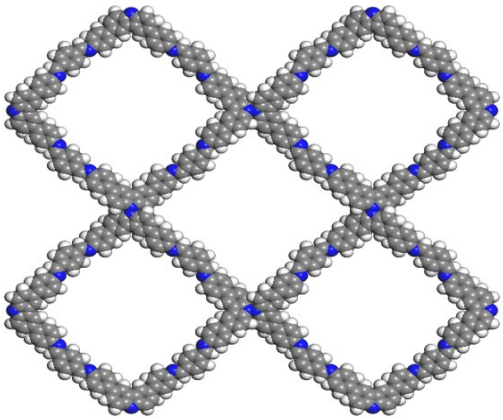	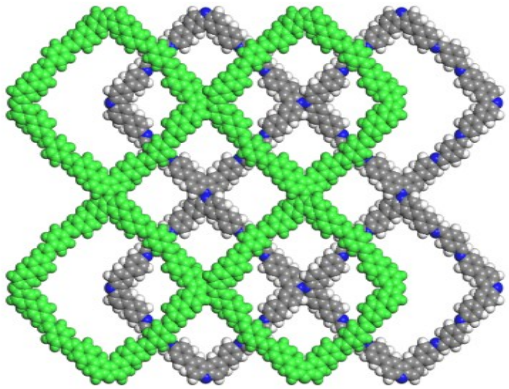
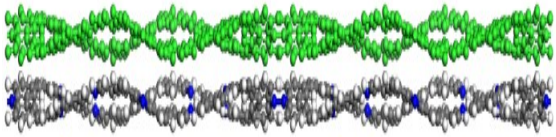	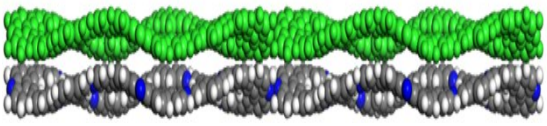

Table S5. Views of space models of BCTB-BCTA COF (a) eclipsed A–A stacking and (b) staggered A–B stacking crystal structure.

(a)	(b)
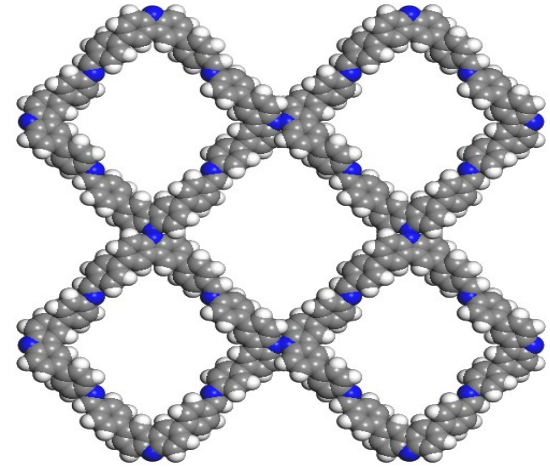	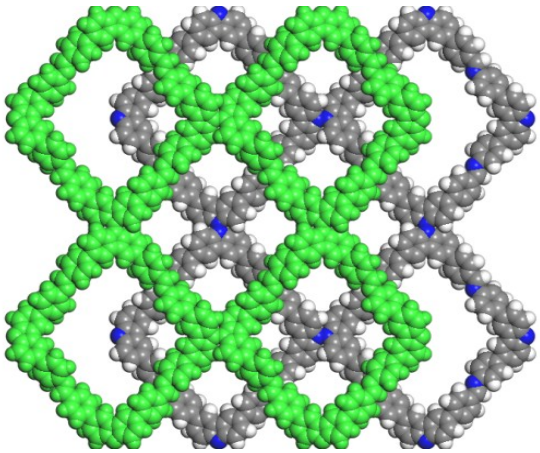
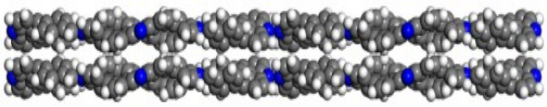	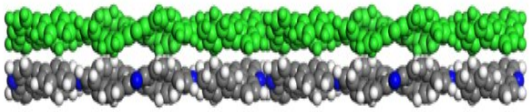

S14. Structural Modeling and Fractional atomic coordinates for COF Structures

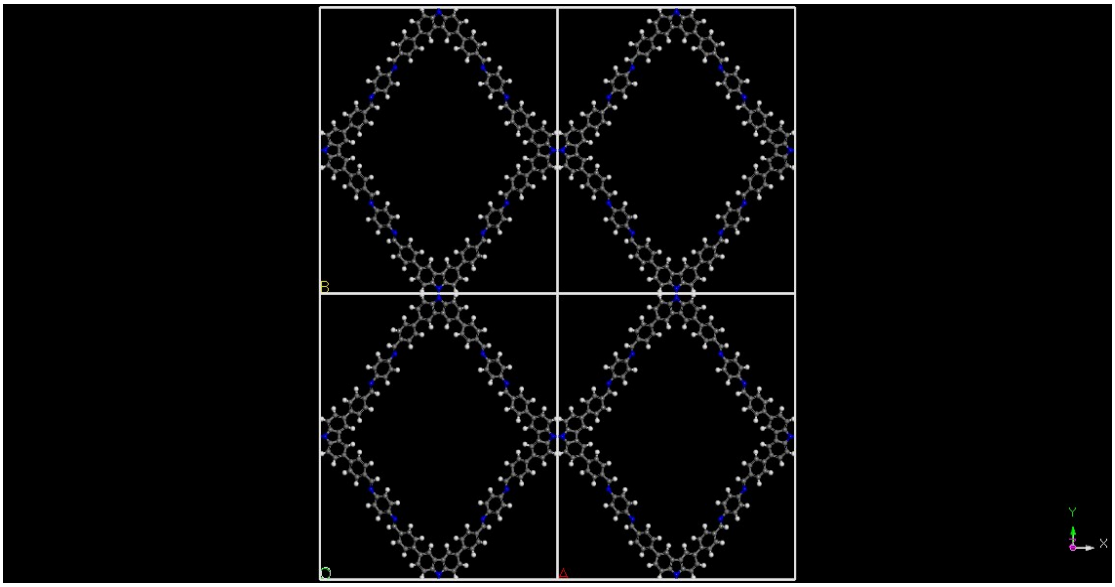

Figure S27. 3D-view of the simulated structure of the BCTB-PD COF along the *c* axis

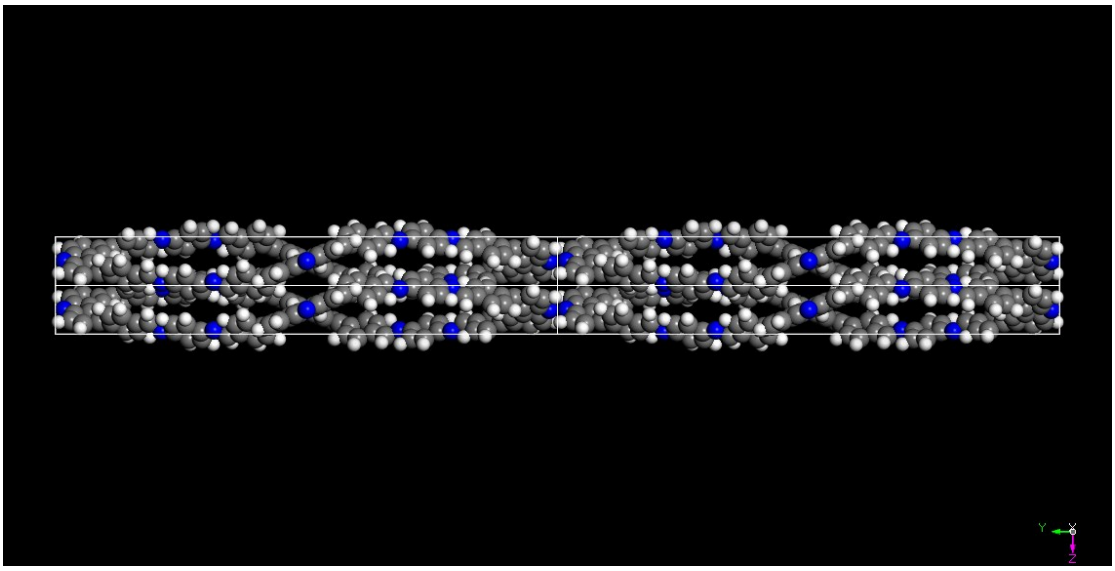

Figure S28. 3D-view of the simulated structure of the BCTB-PD COF along the *a* axis

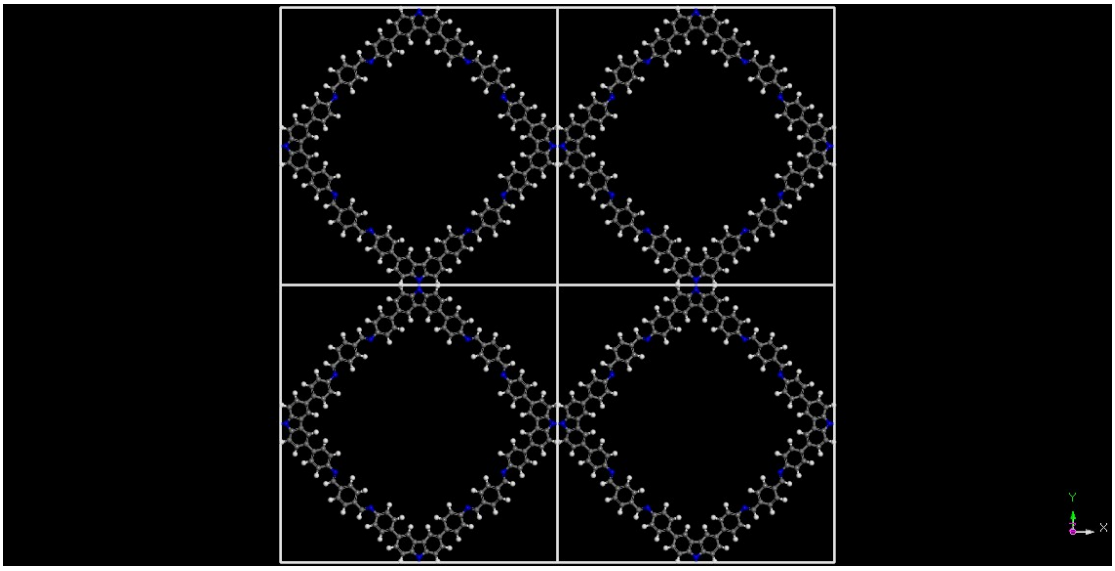

Figure S29. 3D-view of the simulated structure of the BCTA-TP COF along the c axis.

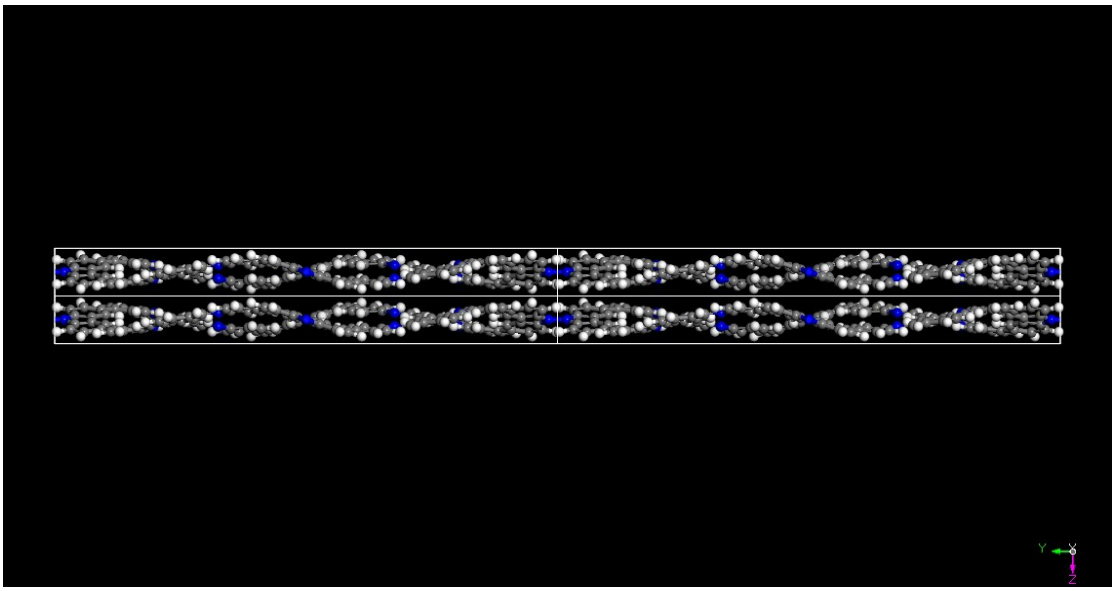

Figure S30. 3D-view of the simulated structure of the BCTA-TP COF along the a axis.

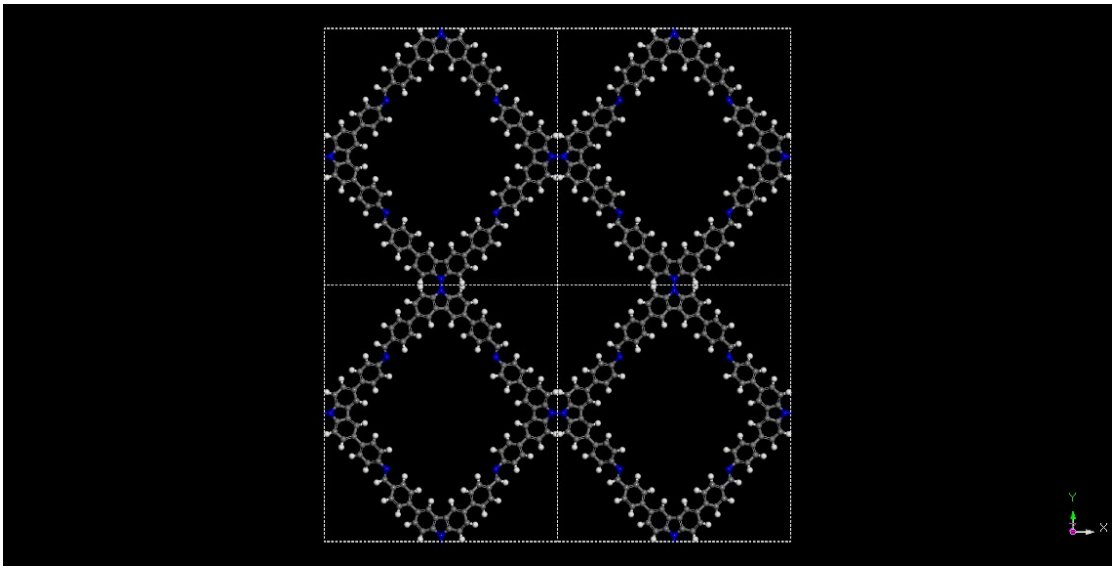

Figure S31. 3D-view of the simulated structure of the BCTB-BCTA COF along the c axis.

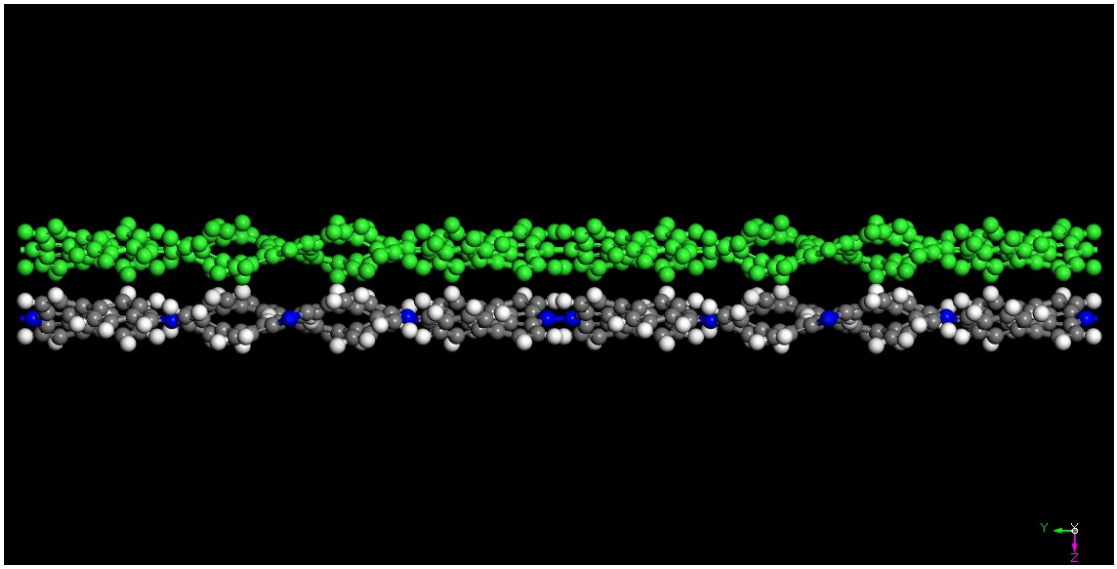

Figure S32. 3D-view of the simulated structure of the BCTB-BCTA COF along the a axis.

Table S6. Fractional atomic coordinates for the unit cell of BCTB-PD COF with A–A stacking.

Sample name: BCTB-PD COF							
Space group: P 2 2 2							
a = 36.10706 Å, b = 42.1182 Å, c = 4.07949 Å, α = β =γ=90°							
R_{wp} = 8.47 %, R_p = 5.67 %							
Atom	***x/a***	***y/b***	***z/c***	**Atom**	***x/a***	***y/b***	***z/c***
C1	0.52758	0.96279	0.59985	H35	0.42879	0.99399	0.24442
C2	0.48245	0.93132	0.43788	H36	0.38520	0.95123	0.11644
C3	0.43760	0.97003	0.27364	H37	0.46697	0.88186	0.41538
C4	0.41267	0.94535	0.20421	H38	0.35378	0.91413	0.51666
C5	0.42264	0.91332	0.25796	H39	0.30735	0.87195	0.50771
C6	0.45864	0.90611	0.36801	H40	0.38107	0.81306	-0.05968
C7	0.39430	0.88808	0.23295	H41	0.42813	0.85555	-0.04778
C8	0.35981	0.89240	0.38518	H42	0.28974	0.81744	0.40379
C9	0.33342	0.86825	0.38192	H43	0.24338	0.78755	0.29812
C10	0.34076	0.83940	0.22343	H44	0.20211	0.74189	0.30521
C11	0.37502	0.83512	0.06570	H45	0.28363	0.68641	-0.20935
C12	0.40178	0.85923	0.07302	H46	0.32591	0.73215	-0.20849
C13	0.31251	0.81414	0.23543	H47	0.24110	0.64908	-0.17595
N14	0.31511	0.78863	0.05684	H48	0.84821	0.33419	0.28603
C15	0.28873	0.76299	0.05254	H49	0.89683	0.3729	0.39635
C16	0.25312	0.76569	0.19076	H50	0.83361	0.4449	-0.10587
C17	0.22910	0.73973	0.19183	H51	0.78458	0.40585	-0.21789
C18	0.23957	0.71083	0.05236	H52	0.94337	0.40303	0.07996
C19	0.27465	0.70824	-0.09582	H53	0.99313	0.43911	0.24500

C20	0.29889	0.73429	-0.09577	H54	0.86216	0.47274	0.38455
N21	0.21380	0.68501	0.07631	N55	0.50000	0.98295	0.50000
C22	0.21697	0.65635	-0.03837	N56	0.98012	0.50000	0.50000
C23	0.81273	0.36704	0.02422				
C24	0.84484	0.35821	0.19623				
C25	0.87272	0.38033	0.25782				
C26	0.86910	0.41182	0.15027				
C27	0.83689	0.42083	-0.01925				
C28	0.80900	0.39854	-0.08360				
C29	0.89892	0.43500	0.22044				
C30	0.93640	0.42614	0.17865				
C31	0.96516	0.44686	0.26671				
C32	0.95663	0.47653	0.39650				
C33	0.91991	0.48514	0.43305				
C34	0.89051	0.46532	0.34624				

Table S7. Fractional atomic coordinates for the unit cell of BCTA-TP-COF with A–A stacking.

Sample name: BCTA-TP COF							
Space group: P 4 2 2							
a = b = 16.2238 Å, c = 3.57625 Å, α = β =γ=90°							
R_{wp} = 7.17% , R_p = 4.74%							
Atom	***x/a***	***y/b***	***z/c***	**Atom**	***x/a***	***y/b***	***z/c***
C1	0.96054	0.47372	0.58893	C17	0.79236	0.76744	0.47017
C2	0.92677	0.51678	0.44704	H18	0.87227	0.46911	0.57227
C3	0.89989	0.46054	0.60745	H19	0.94882	0.39014	0.85294
C4	0.90783	0.42663	0.70751	H20	0.99664	0.43330	0.75659
C5	0.94240	0.41729	0.76217	H21	0.83875	0.43764	0.66816
C6	0.96891	0.44087	0.70660	H22	0.79290	0.39223	0.63661
C7	0.88064	0.59958	0.27556	H23	0.87123	0.31256	0.75219
C8	0.84615	0.40953	0.68518	H24	0.91701	0.35791	0.78817
C9	0.82081	0.38445	0.66677	H25	0.83749	0.71703	0.35871
C10	0.82954	0.34989	0.68518	H26	0.69573	0.35791	0.78817
C11	0.86392	0.34066	0.73095	H27	0.82034	0.77515	0.44626
C12	0.88918	0.36571	0.75057	N28	0.98183	0.50000	0.50000
N13	0.80337	0.67531	0.36032				
C14	0.81003	0.70766	0.38300				
C15	0.73310	0.78312	0.56032				
C16	0.72373	0.74868	0.52970				

Table S8. Fractional atomic coordinates for the unit cell of BCTB-BCTA-COF with A–A stacking.

Sample name: BCTB-BCTA COF							
Space group: P 2 2 2							
a = 28.80335 Å, b = 31.63254 Å, c = 4.04923 Å, α = β =γ=90°							
R_{wp} = 7.47%, R_p = 3.24%							
Atom	***x/a***	***y/b***	***z/c***	**Atom**	***x/a***	***y/b***	***z/c***
C1	0.46498	0.95030	0.59244	C26	0.86262	0.45149	0.40119
C2	0.47756	0.90845	0.55316	H27	0.54299	0.84302	0.46603
C3	0.55340	0.87493	0.40477	H28	0.64616	0.93474	0.16139
C4	0.59957	0.88451	0.31722	H29	0.58977	0.99135	0.24328
C5	0.61133	0.92685	0.24116	H30	0.59649	0.80055	0.13920
C6	0.57906	0.95962	0.28510	H31	0.65654	0.74653	0.23906
C7	0.63652	0.85200	0.34792	H32	0.74542	0.84152	0.66583
C8	0.62879	0.80970	0.25571	H33	0.68564	0.89484	0.57763
C9	0.66290	0.77893	0.31284	H34	0.77630	0.77034	0.58784
C10	0.70522	0.79007	0.46179	H35	0.82396	0.27799	0.67025
C11	0.71316	0.83231	0.54857	H36	0.88294	0.33220	0.59099
C12	0.67914	0.86286	0.49445	H37	0.78210	0.41200	0.10829
C13	0.74200	0.75872	0.52552	H38	0.72251	0.35672	0.19148
N14	0.26632	0.71832	0.47701	H39	0.92833	0.36694	0.16032
C15	0.76909	0.31303	0.42749	H40	0.99056	0.41826	0.24349
C16	0.81472	0.30652	0.53867	H41	0.82748	0.46094	0.46035
C17	0.84846	0.33759	0.49318	N42	0.50000	0.97726	0.50000
C18	0.83735	0.37598	0.33730	N43	0.97503	0.50000	0.50000
C19	0.79153	0.38272	0.22949				

C20	0.75765	0.35143	0.27621				
C21	0.87317	0.40952	0.31228				
C22	0.91971	0.39870	0.23925				
C23	0.95570	0.42805	0.28449				
C24	0.94543	0.46814	0.40698				
C25	0.89945	0.47960	0.44607				

S15. UV-visible spectra of monomers

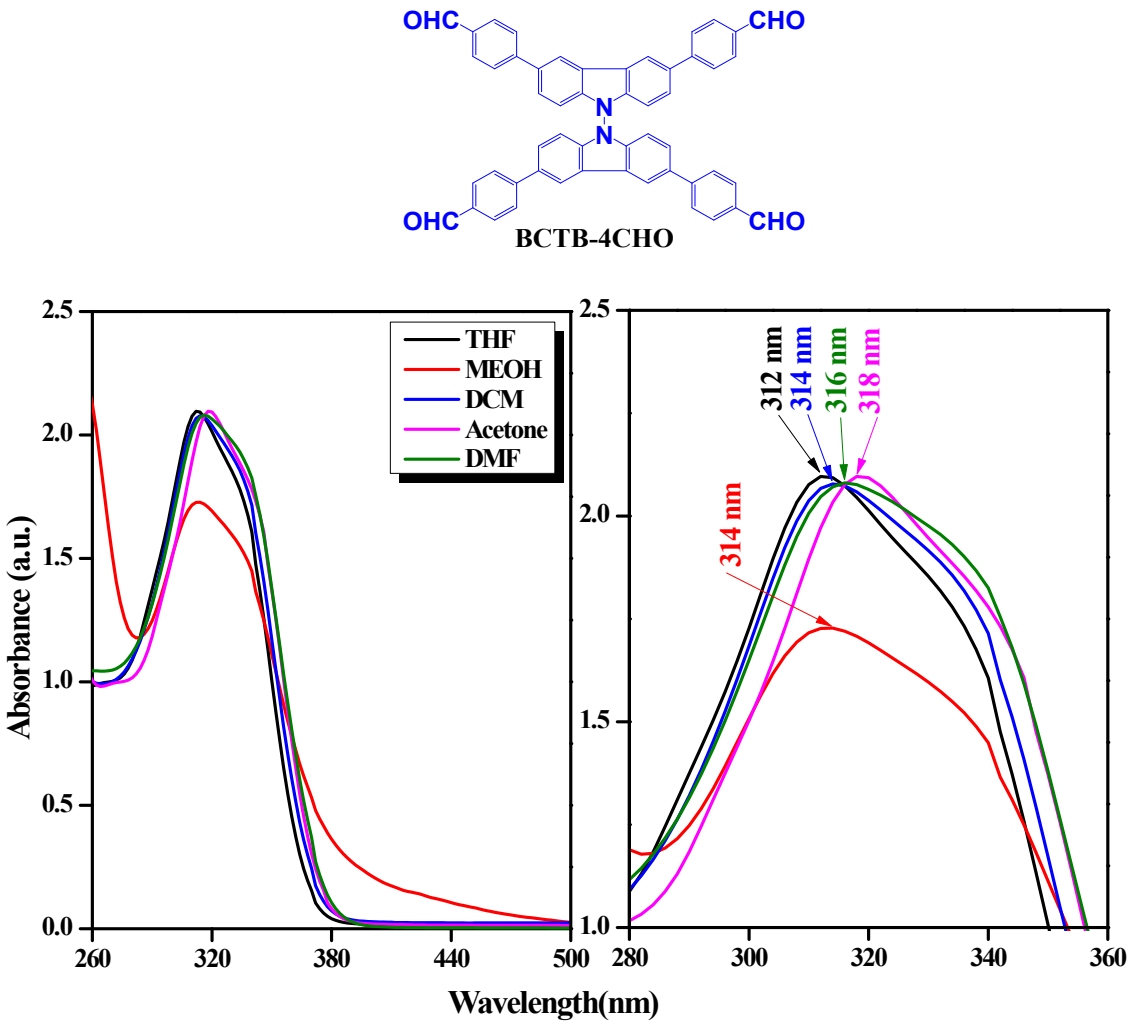

Figure S33. UV-visible spectra of BCTB-4CHO.

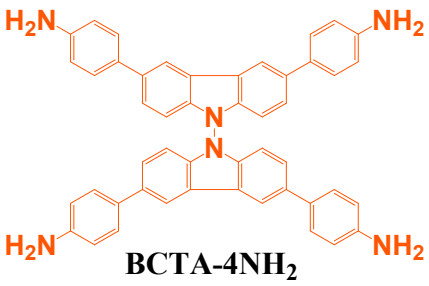

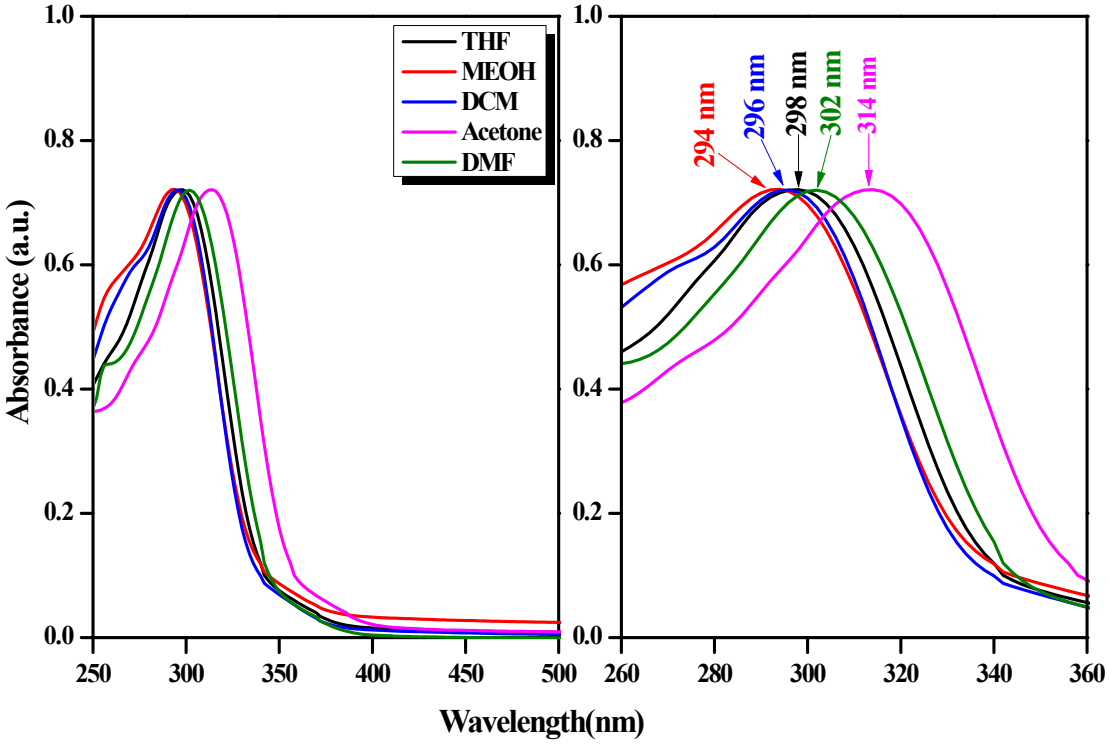

Figure S34. UV-visible spectra of BCTA-4NH_2.

S16. Fluorescence spectra of monomers

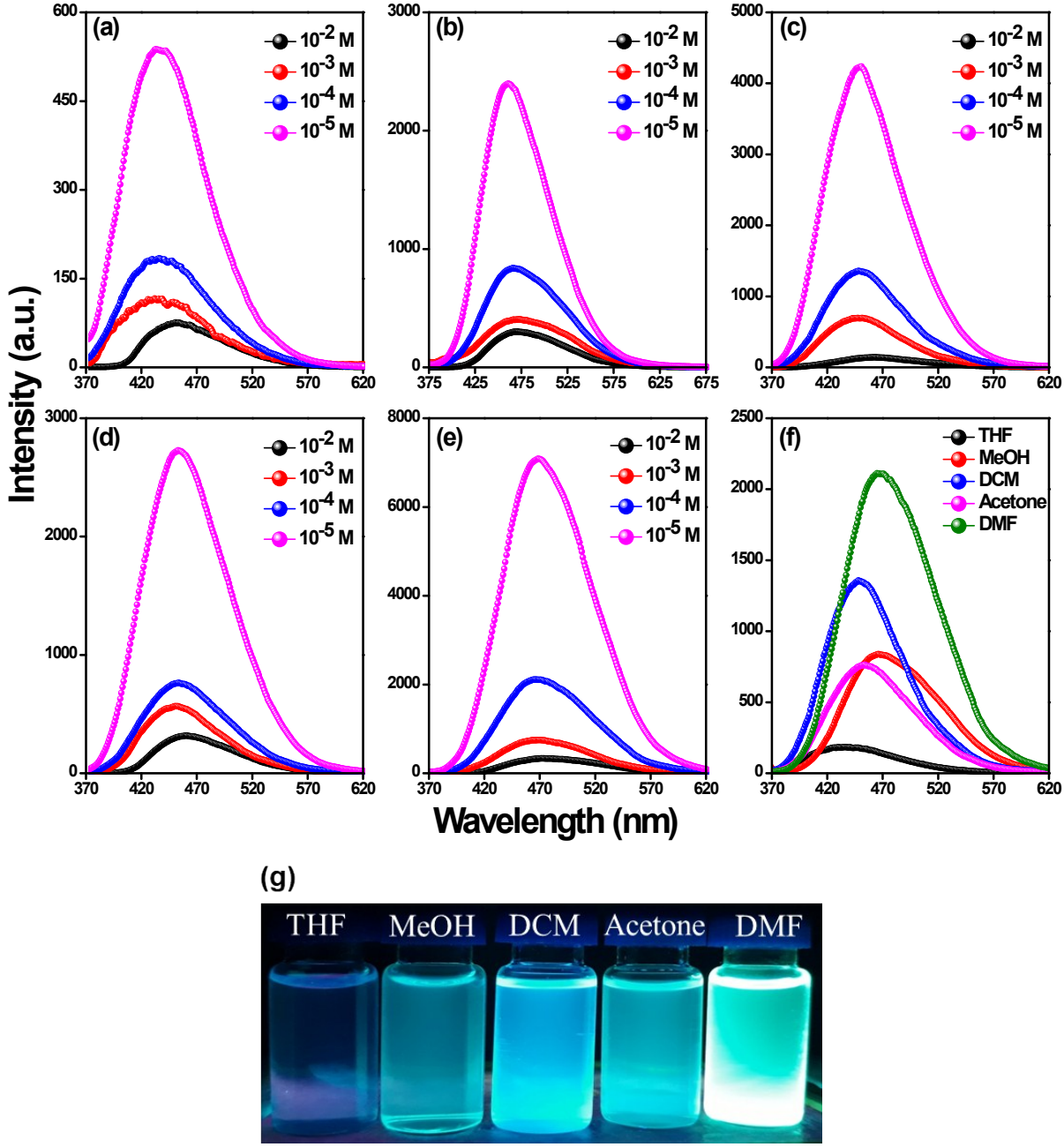

Figure S35. Fluorescence spectra of BCTB-4CHO in (a) THF, (b) MeOH, (c) DCM. (d) acetone, and (e) DMF at different concentrations and (f) their comparison at a concentration of 10^{-4} M under excitation 365 nm. Naked-eye images of (g) BCTB-4CHO dispersed in various solvent at at a concentration of 10^{-4} M under excitation 365 nm.

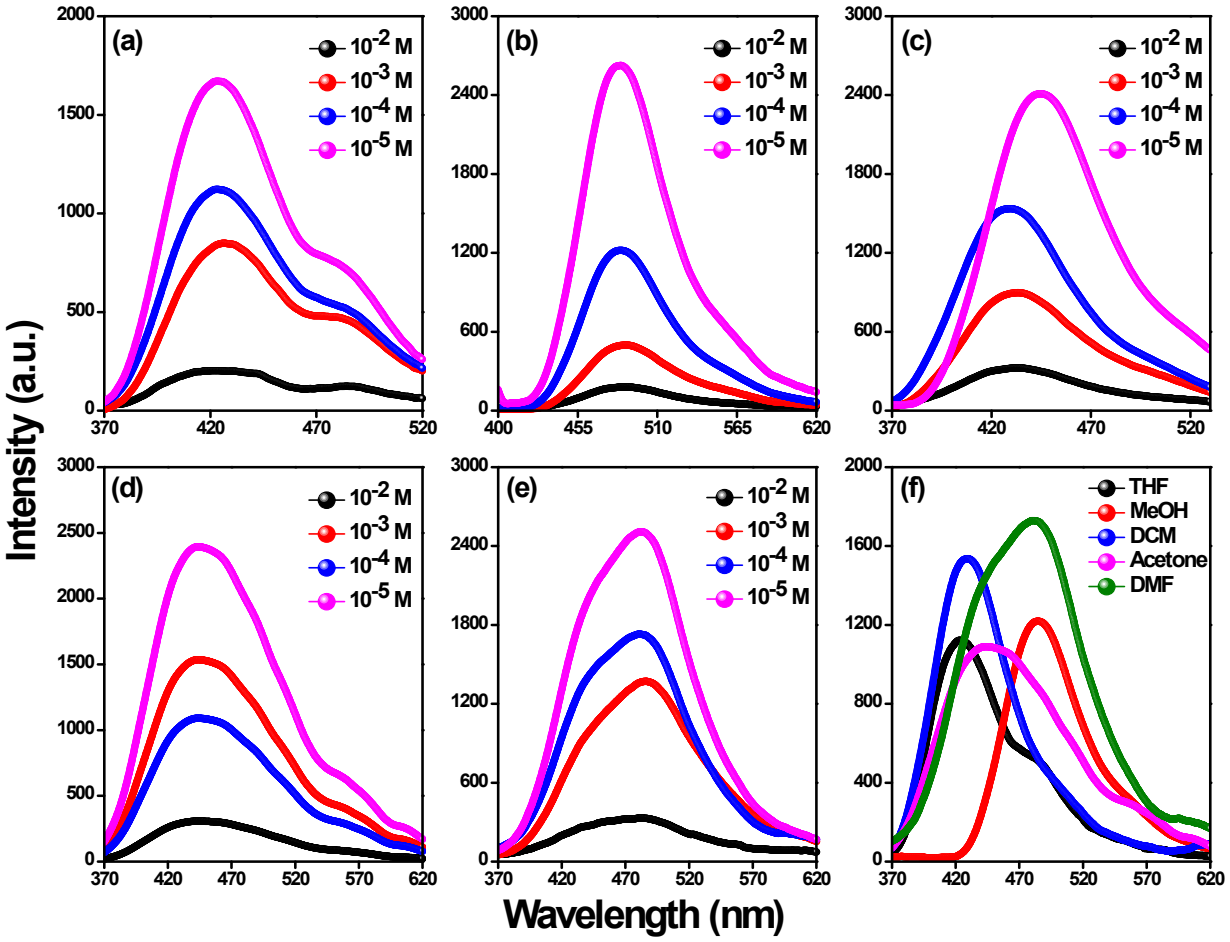

(g)

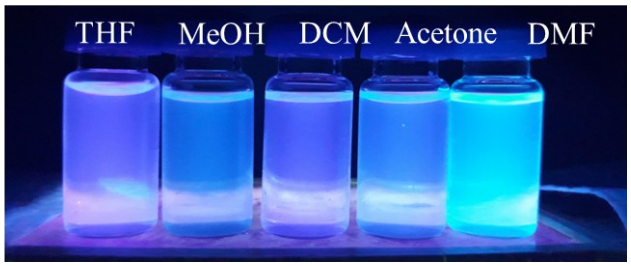

Figure S36. Fluorescence spectra of BCTA-4NH_2 in (a) THF, (b) MeOH, (c) DCM. (d) acetone, and (e) DMF at different concentrations and (f) their comparison at a concentration of 10^{-4} M under excitation 365 nm. Naked-eye images of (g) BCTA-4NH_2 dispersed in various solvent at at a concentration of 10^{-4} M under excitation 365 nm.

S17. Chemical stability of COFs

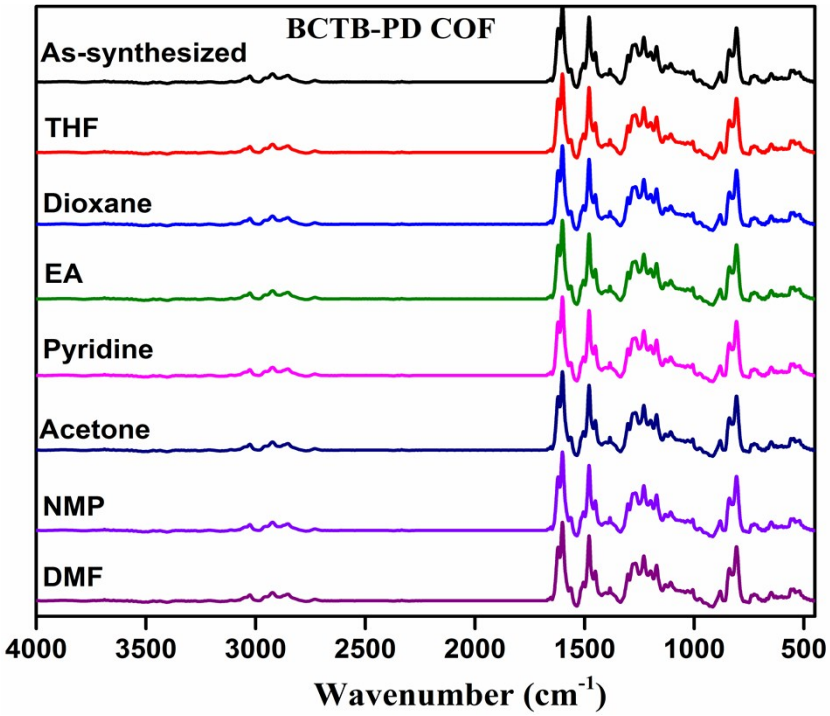

Figure S37. FTIR spectra of BCTB-PD COF as-synthesized and after immersing 3 days in various solvents.

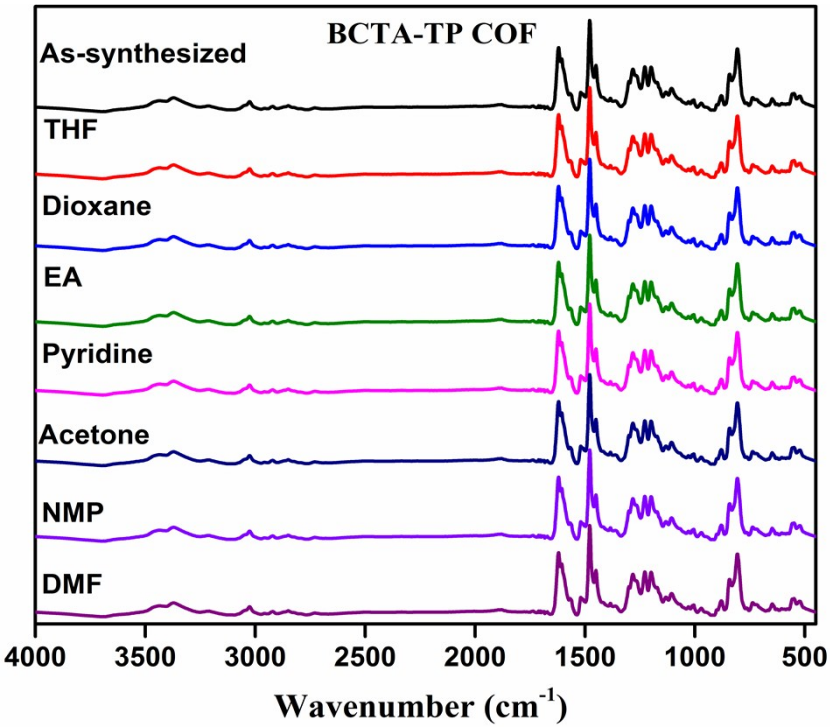

Figure S38. FTIR spectra of BCTA-TP COF as-synthesized and after immersing 3 days in various solvents.

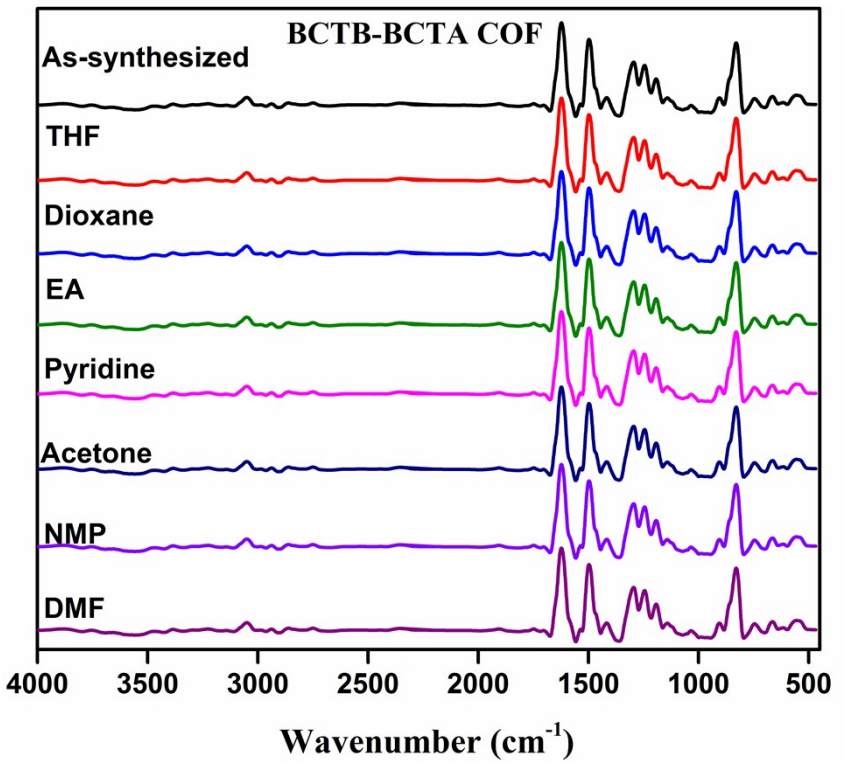

Figure S39. FTIR spectra of BCTB-BCTA COF as-synthesized and after immersing 3 days in various solvents.

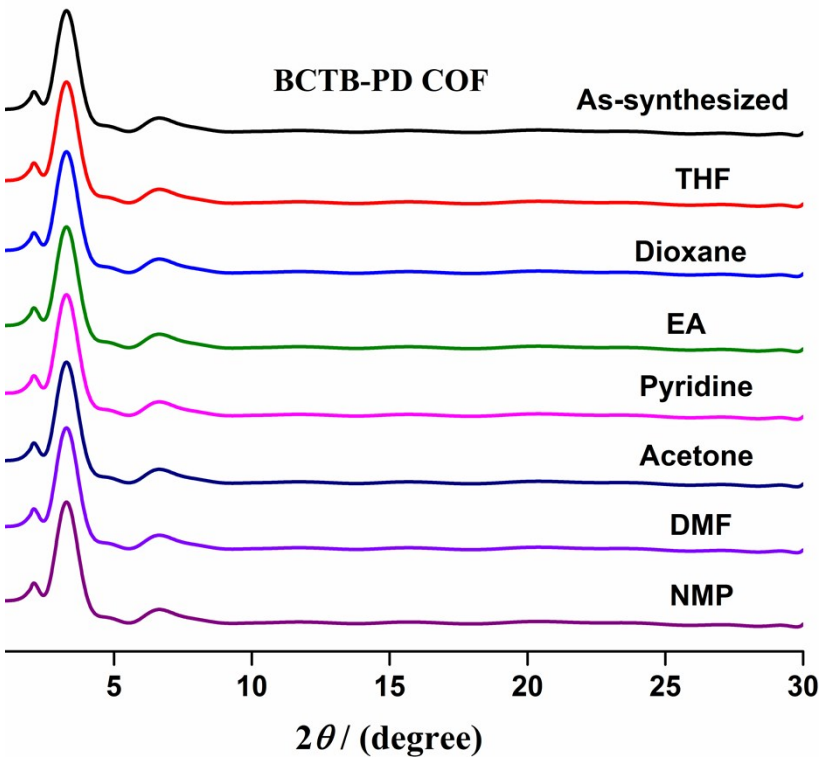

Figure S40. PXRD patterns of BCTB-PD COF as-synthesized and after immersing 3 days in various solvents.

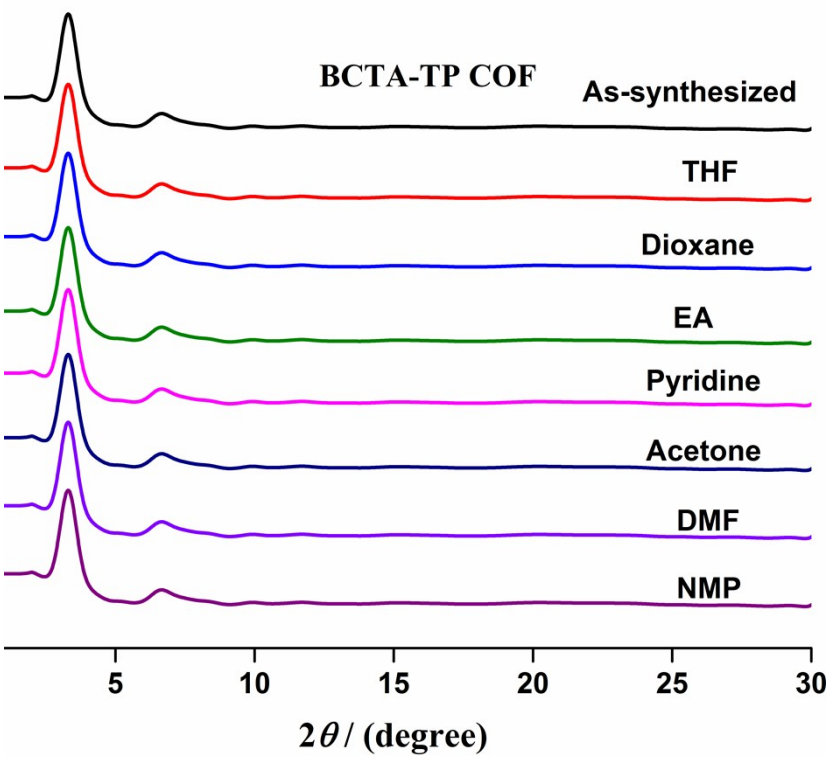

Figure S41. PXRD patterns of BCTA-TP COF as-synthesized and after immersing 3 days in various solvents.

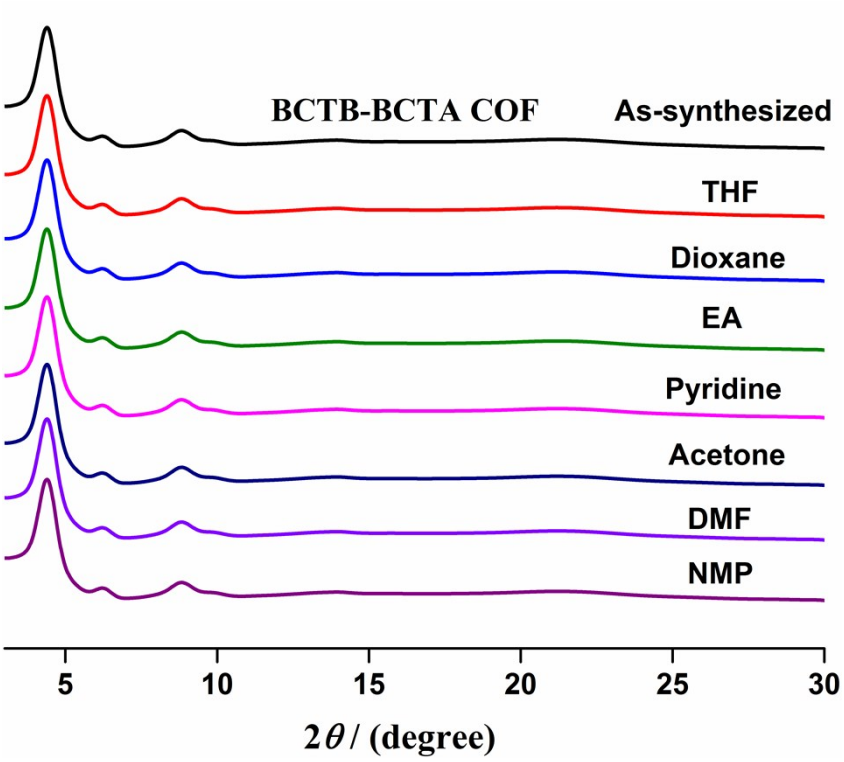

Figure S42. PXRD patterns of BCTB-BCTA COF as-synthesized and after immersing 3 days in various solvents.

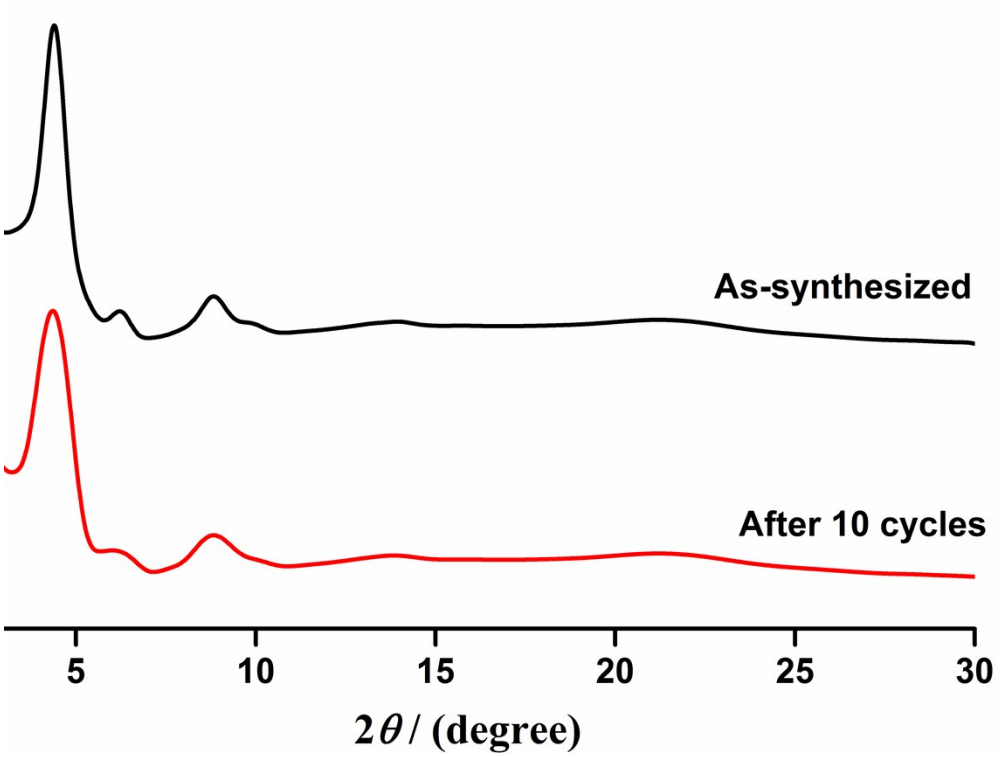

Figure S43. PXRD patterns of BCTB-BCTA COF as-synthesized and after the alternating exposure to HCl and NH_3 vapors for up to 10 cycles.

S18. Fluorescence spectra of COFs and HCl sensing

Table S9. Fluorescence emission maxima and absolute PLQY of COFs.

COFs	Solvent	Emission λ_{max} (nm)	PLQY (%)
BCTB-PD	THF	Very weak fluorscence	0.2
BCTB-PD	Dioxane	423	9.9
BCTB-PD	EA	440	9.6
BCTB-PD	Pyridine	462	12.8
BCTB-PD	Acetone	469	13.5
BCTB-PD	DMF	471	15.9
BCTB-PD	NMP	474	16.3
BCTA-TP	THF	Very weak fluorscence	0.1
BCTA-TP	Dioxane	399	1.1
BCTA-TP	EA	402	0.9
BCTA-TP	Pyridine	420	3.1
BCTA-TP	Acetone	422	3.8
BCTA-TP	DMF	430	5.1
BCTA-TP	NMP	443	5.6
BCTB-BCTA	THF	Very weak fluorscence	0.3
BCTB-BCTA	Dioxane	411	13.8
BCTB-BCTA	EA	437	12.5
BCTB-BCTA	Pyridine	461	17.6
BCTB-BCTA	Acetone	465	19.3
BCTB-BCTA	DMF	472	20.8
BCTB-BCTA	NMP	476	21.2

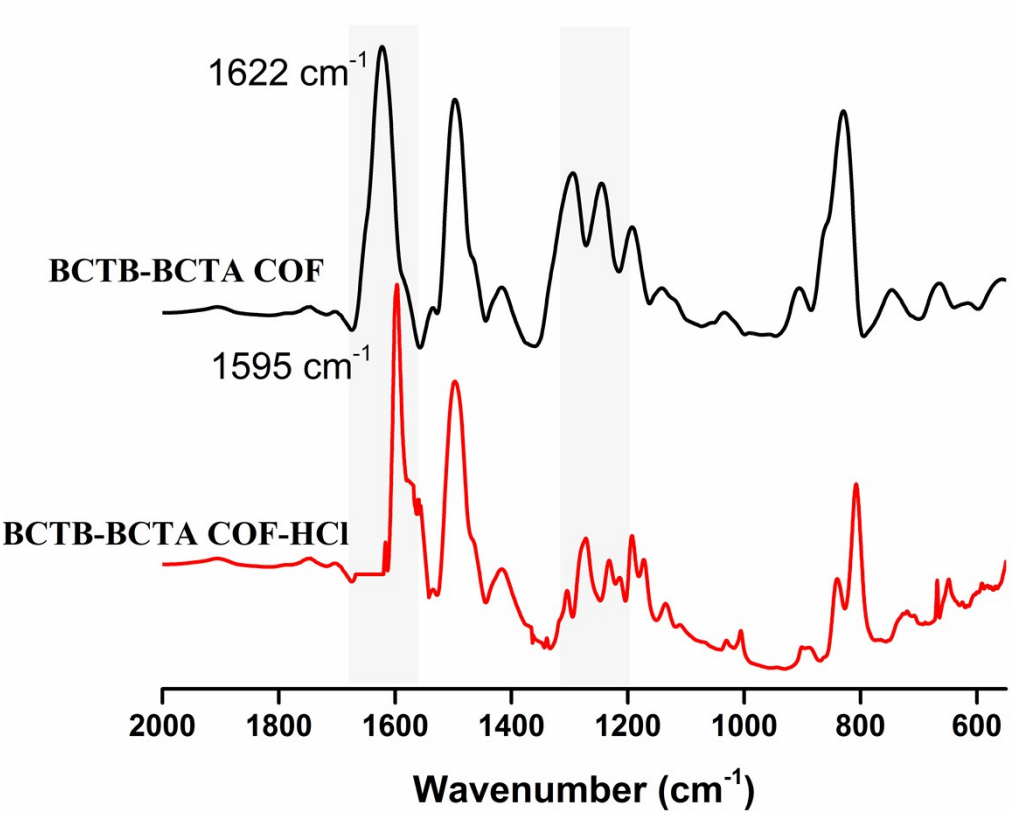

Figure S44. FTIR spectra of BCTB-BCTA COF as-synthesized and after treatment with 1 mmol L^{-1} HCl concentration (BCTB-BCTA COF-HCl).

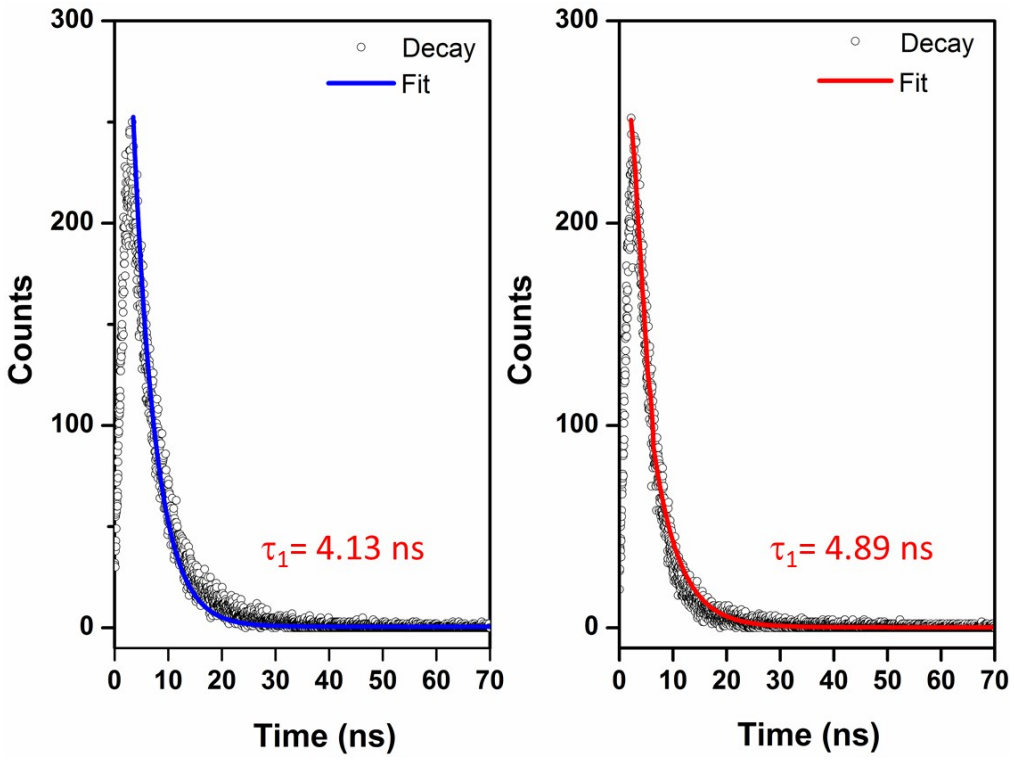

Figure S45. Fluorescence life-time decay of BCTB-BCTA COF as-synthesized and after treatment with 1 mmol L^{-1} HCl concentration (BCTB-BCTA COF-HCl).

S19. References

S1. Xu, T.; Li, Y.; Zhao, Z.; Xing, G.; Chen, L. N, N-Bicarbazole-Based Covalent Triazine Frameworks as High-Performance Heterogeneous Photocatalysts, Macromolecules **2019**, *52*(24), 9786-9791.